

Accepted Manuscript

Design, synthesis, evaluation and molecular modelling studies of some novel 5,6-diphenyl-1,2,4-triazin-3(2*H*)-ones bearing five-member heterocyclic moieties as potential COX-2 inhibitors: A hybrid pharmacophore approach

Anupam G. Banerjee, Nirupam Das, Sushant A. Shengule, Piyooosh A. Sharma, Radhey Shyam Srivastava, Sushant Kumar Shrivastava

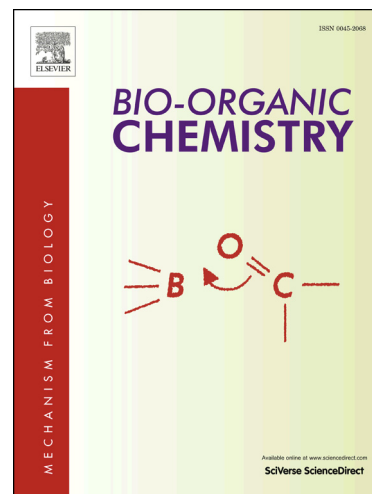
PII: S0045-2068(16)30239-5
DOI: <http://dx.doi.org/10.1016/j.bioorg.2016.10.003>
Reference: YBIOO 1958

To appear in: *Bioorganic Chemistry*

Received Date: 1 September 2016
Revised Date: 7 October 2016
Accepted Date: 8 October 2016

Please cite this article as: A.G. Banerjee, N. Das, S.A. Shengule, P.A. Sharma, R. Shyam Srivastava, S. Kumar Shrivastava, Design, synthesis, evaluation and molecular modelling studies of some novel 5,6-diphenyl-1,2,4-triazin-3(2*H*)-ones bearing five-member heterocyclic moieties as potential COX-2 inhibitors: A hybrid pharmacophore approach, *Bioorganic Chemistry* (2016), doi: <http://dx.doi.org/10.1016/j.bioorg.2016.10.003>

This is a PDF file of an unedited manuscript that has been accepted for publication. As a service to our customers we are providing this early version of the manuscript. The manuscript will undergo copyediting, typesetting, and review of the resulting proof before it is published in its final form. Please note that during the production process errors may be discovered which could affect the content, and all legal disclaimers that apply to the journal pertain.



Design, synthesis, evaluation and molecular modelling studies of some novel 5,6-diphenyl-1,2,4-triazin-3(2H)-ones bearing five-member heterocyclic moieties as potential COX-2 inhibitors: A hybrid pharmacophore approach

Anupam G. Banerjee^a, Nirupam Das^{a,b}, Sushant A. Shengule^c, Piyooosh A. Sharma^a,
Radhey Shyam Srivastava^a, Sushant Kumar Shrivastava^{a*}

*^aPharmaceutical Chemistry Research Laboratory, Department of Pharmaceutics
Indian Institute of Technology (Banaras Hindu University), Varanasi – 221 005 (India)*

^bDepartment of Pharmaceutical Sciences, Assam University, Silchar – 788 011, (India)

^cNational Toxicology Centre, Vadgaon Khurd, Sinhagad Road, Pune – 411 041 (India)

*Address correspondence to:

Dr. Sushant Kumar Shrivastava

Professor

Department of Pharmaceutics

Indian Institute of Technology (BHU), Varanasi- 221 005, India

Email: skshrivastava.phe@iitbhu.ac.in; agbanerjee.rs.phe@iitbhu.ac.in

Phone: +91-542-6702725

Abstract:

A series of novel hybrids comprising of 1,3,4-oxadiazole/thiadiazole and 1,2,4-triazole tethered to 5,6-diphenyl-1,2,4-triazin-3(2*H*)-one were designed, synthesised and evaluated as COX-2 inhibitors for the treatment of inflammation. The synthesised hybrids were characterised using FT-IR, ¹H-NMR, ¹³C-NMR, elemental (C,H,N) analyses and assessed for their anti-inflammatory potential by *in vitro* albumin denaturation assay. Compounds exhibiting activity comparable to indomethacin and celecoxib were further evaluated for *in vivo* anti-inflammatory activity. Oral administration of promising compounds **3c-3e** and **4c-4e** did not evoke significant gastric, hepatic and renal toxicity in rats. These potential compounds exhibited reduced malondialdehyde (MDA) content on the gastric mucosa suggesting their protective effects by inhibition of lipid peroxidation. Based on the outcome of *in vitro* COX assay, compounds **3c-3e** and **4c-4e** (IC₅₀ 0.60 µM-1.11 µM) elicited an interesting profile as competitive selective COX-2 inhibitors. Further, selected compounds **3e** and **4c** were found devoid of cardiotoxicity post evaluation on myocardial infarcted rats. The *in silico* binding mode of the potential compounds into the COX-2 active site through docking and molecular dynamics exemplified their consensual interaction and subsequent COX-2 inhibition with significant implications for structure-based drug design.

Keywords: Molecular hybridisation; COX-2; 1,2,4-triazine; 1,3,4-oxadiazole; 1,3,4-thiadiazole; cardiotoxicity.

1. Introduction

Inflammation is a multifaceted process reflecting the response of a host, either localised or more generalised to various noxious stimuli. Pathogenesis of many mechanistically related disorders such as arthritis, carcinogenesis, neurodegeneration and autoimmune diseases are attributed directly or indirectly to an inflammatory response. Non-steroidal anti-inflammatory drugs (NSAIDs) are the mainstay of the therapeutic intervention of inflammation and pain. The key mechanism by which NSAIDs exert their anti-inflammatory activity is through inhibition of cyclooxygenase (COX) derived prostaglandin synthesis, but the long term use of these drugs are restricted due to gastrointestinal [1], renal [2], and hepatic side effects [3]. As a result, selective COX-2 inhibitors, such as celecoxib, rofecoxib, parecoxib and valdecoxib, were designed to surmount the gastric injury associated with classical NSAIDs. However, the cardiovascular risk related to "-coxibs" has resulted in a voluntary withdrawal of rofecoxib (Vioxx[®]) and valdecoxib (Bextra[®]) from the market [4]. Therefore, the challenge persists, to address the unmet medical need by developing effective anti-inflammatory agents with enhanced safety profile.

Synthesis of nitrogen-containing heterocyclic compounds has been attracting increasing interest because of their utility for targeting various biological receptors with a high degree of binding affinity [5]. The 1,2,4-triazine nucleus is considered an important chemical synthon exhibiting a broad range of therapeutic activities including COX-2 inhibition [6, 7] and anticancer activities [8]. An array of established biological activities associated with the 1,2,4-triazine nucleus ensures that the synthesis of novel chemical entities (NCE's) containing this critical ring system remains a topic of current interest [9]. Our interest on the 1,2,4-triazine nucleus has stemmed from the fact that apart from azapropazone, which is available only in some parts of Europe, no other NSAID consisting of the central 1,2,4-triazine heterocycle is currently available in the market. Azapropazone now stands discontinued in the British National Formulary (BNF). It is an anti-inflammatory, analgesic, antipyretic and a potent uricosuric agent used in the treatment of rheumatoid arthritis, osteoarthritis, ankylosing spondylitis, and gout. Its use is marred by the gastrointestinal side-effects such as nausea, epigastric pain, and dyspepsia. However, the use of azapropazone is restricted only to cases where other NSAID's have failed [10].

Compounds containing 1,3,4-oxadiazole have been marked with exceptional chemical behaviour with a plethora of varied biological activities reported in the literature [11]. They have also stirred interest as potential bioisosteres for carboxylic acids, esters, and carboxamides [12]. A number of molecules based upon substituted 1,3,4-oxadiazoles template have been investigated for their COX-2 inhibitory effects [13-16].

Further, it is reported that the compact and a highly polarizable 1,3,4-thiadiazole mesoionic system can easily permeate through cellular membranes to interact with diverse biological targets with distinct COX-2 inhibitory activity [17-21]. 1,2,4-triazoles and their derivatives are also reported to exhibit an array of potential therapeutic properties [22] and due to the polar nature of triazole ring, it significantly improves the pharmacological profile by improving the solubility of the drug [23]. There is an extensive literature on 1,2,4-triazole derivatives reported possessing selective COX-2 inhibitory property [24-26].

1.1. Designing Considerations

In our quest for seeking potential COX-2 inhibitors with superior safety profile, we had previously explored the 5,6-diphenyl-1,2,4-triazine and the 1,3,4-oxadiazole nucleus by incorporating it into a single pharmacophore matrix. Our aim was to establish and investigate the synergistic benefits of the synthesised molecules for anti-inflammatory and analgesic activity. During our experiments, it ushered upon us that such an approach resulted in promising anti-inflammatory and analgesic effects and further investigation on their mechanism of action indicated that the promising derivatives preferentially inhibited COX-2 in a competitive manner at a micromolar concentration (3.07-3.23 μM) [27]. These findings were further corroborated by computer aided drug design tools such as *in silico* molecular docking and molecular dynamics studies.

Thus taking a cue from the favourable biological profile as COX-2 inhibitors, the 1,2,4-triazine and 1,3,4-oxadiazole nucleus were once again selected as the framework for designing of new hybrids. Moreover, accumulating lines of evidence suggest that hybridisation of two or more diverse bioactive molecules with corresponding pharmacophoric functions or with different mechanisms of action renders synergistic effects contributing to the overall activity profile of the molecule [28-32]. Further, it was decided to swap the 1,3,4-oxadiazole nucleus with its bioisosteric replacement of 1,3,4-thiadiazole and 1,2,4-triazole and assess the effects of such substitution on the selective COX-2 inhibition profile of the compounds.

On the basis of these promising outcome and in continuation of our research endeavour towards the development of safer anti-inflammatory agents [33, 34], we have reported herein the design and synthesis of some new 5,6-diphenyl-1,2,4-triazin-3(2*H*)-ones assembled into a structural hybrid with the 5-substituted 1,3,4-oxadiazole/thiadiazole or 1,2,4-triazole nucleus.

The hybrids were developed in conformation with the structural prerequisites for selective COX-2 inhibitory activity. It consisted of a diaryl composition which is reported to play a crucial role in

anchoring the molecule within the COX-2 active site through hydrophobic interaction [14]. The diaryl structural moiety was attached to a central 1,2,4-triazine ring thereby giving rise to a diaryl heterocyclic skeleton as observed in selective COX-2 inhibitors from the diaryl heterocycle series (e.g. celecoxib, rofecoxib, valdecoxib, and etoricoxib). This basic skeleton was then hybridised *via* a methylene linker with substituted five-membered heterocycles with the aim of imparting flexibility to the overall hybridised structure (**Fig. 1**).

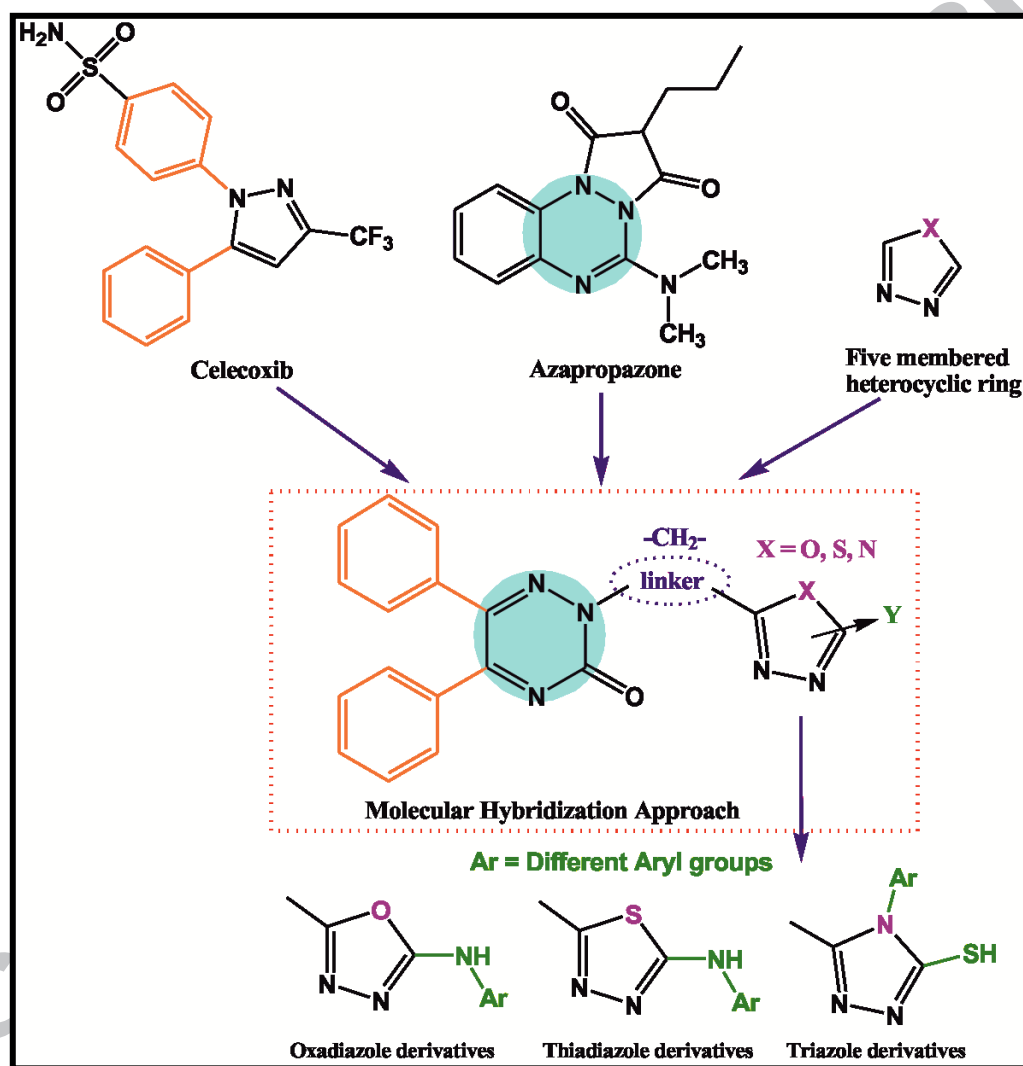


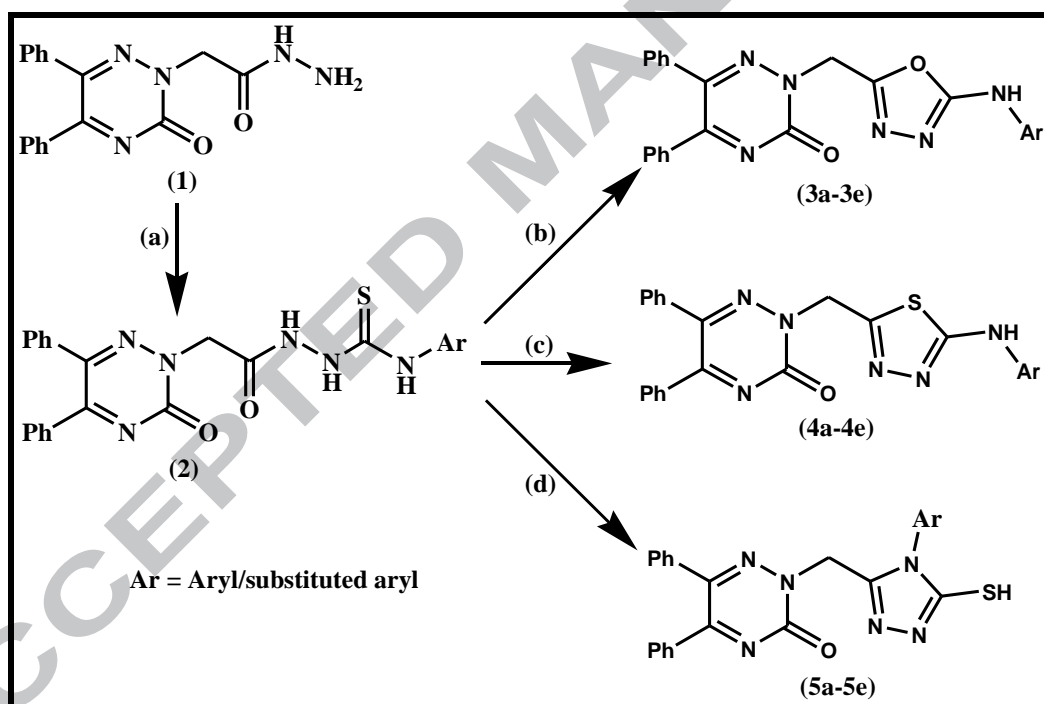
Fig. 1. Design strategy for the compounds **3a-3e**, **4a-4e** and **5a-5e** using molecular hybridisation approach.

The outcome of the design approach was supported by *in vitro* and *in vivo* bioassay models. Further, the relative safety profile of the promising compounds to the standard drugs was evaluated concerning gastric, hepatic, renal and cardiac parameters. Finally, their consensual binding mode to the COX-2 active site was validated by *in silico* docking and binding stability assessed using molecular dynamics studies.

2. Results and discussion

2.1. Chemistry

The target compounds were synthesised as per the reaction sequence outlined in **Scheme 1**. Treatment of 2-(3-oxo-5,6-diphenyl-1,2,4-triazin-2(3*H*)-yl)acetohydrazide (**1**) with various aryl isothiocyanates in ethanol yielded the corresponding aryl thiosemicarbazides (**2a-2e**). The structure of thiosemicarbazides was confirmed by their FT-IR spectrum which displayed absorption peaks at 3288-3109 cm^{-1} for NH, 1608-1699 cm^{-1} for C=O and 1192-1205 cm^{-1} corresponding to C=S stretching vibrations. The ^1H NMR spectrum showed a multiplet at $\delta = 7.08$ -8.23 for the aromatic protons. The CSNH and CONH protons were observed as a singlet at $\delta = 9.96$ -9.71 ppm and $\delta = 10.63$ -10.51 ppm, respectively confirming the formation of thiosemicarbazide. The unique presence of C=S bond was also confirmed by ^{13}C NMR whereby it elicited a downfield signal at $\delta = 180$ -182 ppm for the carbon linked to sulphur.



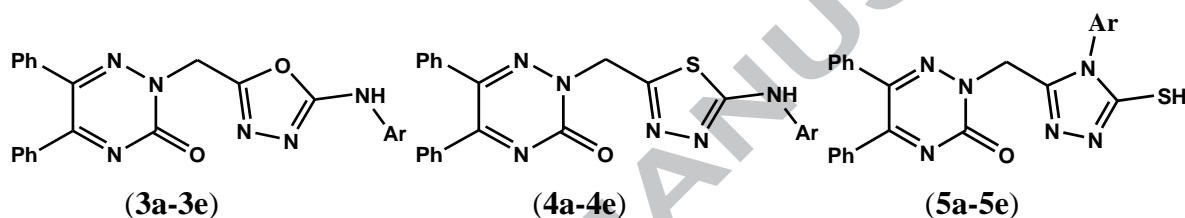
Scheme 1 Synthesis of target compounds: (a) phenyl/substituted phenyl isothiocyanate, Ethanol (75% v/v), Reflux 6 h (b) KI/I_2 , aq. NaOH (5N), Reflux 1h (c) cold H_2SO_4 , Stirring 4-6 h (d) aq. NaOH (4N), Reflux 2 h.

The thiosemicarbazides (**2a-2e**) were oxidatively cyclized to 5-arylamino-1,3,4-oxadiazole compounds (**3a-3e**) by the elimination of H_2S using iodine and potassium iodide in ethanolic NaOH. The FT-IR spectra showed a characteristic absorption peak at 3403-3363 cm^{-1} and 1593-1548 cm^{-1} attributed to N-H and C=N stretching vibration, respectively. The structures were further supported by ^1H NMR spectra which showed a multiplet at $\delta = 8.41$ -6.88 ppm accounting for the aromatic protons. The disappearance of CONH and CSNH singlet signals of thiosemicarbazides

(**2a-2e**) and the retention of NH signal at $\delta = 8.43-8.33$ ppm confirmed the formation of oxadiazole ring.

The 5-arylamino-1,3,4-thiadiazole compounds (**4a-4e**) were obtained by cyclisation of (**2a-2e**) after treating it with cold concentrated sulphuric acid. The FT-IR spectrum showed an absorption peak at $1599-1527\text{ cm}^{-1}$ marking the presence of C=N stretching vibrations. Singlet corresponding to CONH and CSNH protons were absent in the ^1H NMR spectrum, and a multiplet confirming the existence of aromatic protons was observed in region $\delta = 8.40-6.94$ ppm. Apart from this, the NH protons were found as a singlet at $\delta = 8.42-8.36$ ppm establishing the structure of the compounds.

Table 1 Chemical structures and physicochemical properties of the synthesised compounds



Compound	Ar	R _f [*]	mp (°C)	Log P ^{**}
3a	Phenyl	0.40	229-231	3.44
3b	4-Methylphenyl	0.39	235-237	3.98
3c	4-Methoxyphenyl	0.35	246-248	4.00
3d	4-Chlorophenyl	0.33	244-245	4.19
3e	4-Nitrophenyl	0.45	255-257	3.89
4a	Phenyl	0.39	232-233	4.32
4b	4-Methylphenyl	0.42	240-242	4.45
4c	4-Methoxyphenyl	0.38	247-248	4.38
4d	4-Chlorophenyl	0.35	252-254	4.58
4e	4-Nitrophenyl	0.42	263-265	4.37
5a	Phenyl	0.41	237-239	3.72
5b	4-Methylphenyl	0.40	248-250	4.17
5c	4-Methoxyphenyl	0.39	257-259	3.93
5d	4-Chlorophenyl	0.38	258-260	4.30
5e	4-Nitrophenyl	0.44	269-271	3.72

*R_f (Solvent system): DCM/Methanol (9.5:0.5)

** Log P value was determined using shake flask method.

Lastly, the thiosemicarbazides (**2a-2e**) on heating with ethanolic 4 N NaOH underwent cyclisation through dehydration to afford the 1-aryl-5-mercapto-1,2,4-triazole compounds (**5a-5e**). The formation of the 1,2,4-triazole ring was supported by its ^1H NMR spectrum which showed a singlet corresponding to SH proton at $\delta = 11.31-11.26$ ppm in addition to the aromatic protons at $\delta = 8.20-$

6.46 ppm. All other ^{13}C NMR peaks were observed as per the expected chemical shift. The results of the elemental analyses were within $\pm 0.4\%$ of theoretical values. The partition coefficient (Log P) was determined in n-octanol/water by "shake-flask" method. The R_f values, melting point and Log P values of the title compounds are presented in **Table 1**.

2.2. Pharmacology

2.2.1. In-vitro albumin denaturation assay

The albumin denaturation assay is a quick and inexpensive method, which seeks to limit the use of animals in the initial drug discovery process [35]. Denaturation of tissue proteins is one of the well-documented causes of inflammatory and arthritic diseases [36]. Furthermore, NSAID's like indomethacin and celecoxib are reported to inhibit the denaturation of proteins [37, 38]. Therefore, substances that can avert protein denaturation would be worthwhile for anti-inflammatory drug development since denaturation of protein could be the initial step for further protein modifications like glycosylation which has been reported in chronic inflammatory disorders [39].

Table 2 Albumin denaturation assay (*in vitro* screening)

Compound	Absorbance	% inhibition	Compound	Absorbance	% inhibition
Control	0.1258 \pm 0.0079	--	4b	0.2102 \pm 0.0184 ^a	67.10
Indo	0.2298 \pm 0.0184 ^a	82.67	4c	0.2235 \pm 0.0132 ^a	77.66
Celecoxib	0.2268 \pm 0.0166 ^a	80.29	4d	0.2228 \pm 0.0108 ^a	77.11
3a	0.2046 \pm 0.0125 ^a	62.64	4e	0.2237 \pm 0.0204 ^a	77.82
3b	0.2049 \pm 0.0110 ^a	62.88	5a	0.1896 \pm 0.0162	50.71
3c	0.2240 \pm 0.0148 ^a	78.06	5b	0.1913 \pm 0.0128	52.07
3d	0.2249 \pm 0.0173 ^a	78.77	5c	0.1952 \pm 0.0117	55.17
3e	0.2255 \pm 0.0109 ^a	79.25	5d	0.2163 \pm 0.0202 ^a	71.94
4a	0.2040 \pm 0.0146 ^a	62.16	5e	0.2165 \pm 0.0180 ^a	72.10

Values are expressed as the mean \pm S.D (n = 3).

a: p < 0.05 vs. Control

All compounds and standard drugs were taken at a dose of 0.0279 mmol.

The results of the initial screening of all the synthesised compounds by albumin denaturation assay are shown in **Table 2**. Protein stabilisation by the compounds (**3a-3e**, **4a-4e**, **5a-5e**) was indicated by the test compounds and standard drugs (indomethacin and celecoxib) compared to the control. Hybrids **3c-3e**, **4c-4e**, **5d** and **5e** exhibited inhibition (71.94%-79.25%) as compared to the standard drugs indomethacin (82.67%) and celecoxib (80.29%), respectively. Compounds failing to elicit a minimum of 70% inhibition of protein denaturation compared to the "control" were dropped from the further evaluation process.

2.2.2. Acute oral toxicity studies

The acute toxicity determination for compounds **3c-3e**, **4c-4e**, **5d** and **5e** was performed as per OECD 423 guidelines (OECD 423-2002) on healthy nulliparous female rats. All of the tested compounds were well tolerated up to a dose of 500 mg kg⁻¹. Also, no mortality was observed 14 days post administration, even at the highest evaluated dose of 500 mg kg⁻¹ body weight thereby suggesting a significant margin of safety.

2.2.3. Carrageenan induced rat paw oedema

Carrageenan is widely used to induce an acute inflammatory response in a pre-clinical screening of compounds for the assessment of their anti-inflammatory potential. This phlogistic agent causes a severe inflammatory response apparent within 30 min when locally injected into the sub-plantar region of the rat paw [40]. Carrageenan-induced paw oedema is a biphasic event, which mimics the exudative stage of inflammation, one of the important processes of inflammatory pathology [41]. The release of pro-inflammatory agents like histamine, serotonin, and similar substances occurs in the early phase (till 2 h); and the later stage (3 h post treatment) is associated with the activation of prostaglandins [42]. The outcome of the anti-inflammatory effects of the compounds **3c-3e**, **4c-4e**, **5d** and **5e** are presented in **Table 3**. With the exception of hybrids **5d** and **5e**, all the evaluated compounds exhibited marked inhibition of the oedema in comparison to the standard drugs indomethacin and celecoxib, respectively. Since the maximal anti-inflammatory effect was detected at 5 h, this was made the basis of discussion.

From the results portrayed in **Table 3**, it is apparent that compounds **3d** and **3e** possessed a fast onset of action (post 2 h) as compared to others. Amongst the eight evaluated compounds, six were found to exhibit anti-inflammatory activity (57.90%-61.56% reduction in inflammation). Compound **3e** bearing an electron withdrawing 4-nitrophenyl group on the five-member 1,3,4-oxadiazole ring elicited excellent protection against inflammation (61.56%) compared to standard drugs indomethacin (63.56%) and celecoxib (62.26%), respectively. It was followed by **3d** (60.97%) and **3c** (60.85%), also bearing electron withdrawing groups 4-chlorophenyl and 4-methoxyphenyl on the oxadiazole ring. Compounds **4c-4e** bearing a bioisosteric replacement of the 1,3,4-oxadiazole with a 1,3,4-thiadiazole ring bearing an electron withdrawing substituent at the para position exhibited good (59.20%-58.49%) anti-inflammatory effect. Compounds **3c-3e** and **4c-4e** were seen to possess comparable anti-inflammatory effect in the late phase (post 2 h) of the bioassay model with respect to the standard drugs, thereby deserving further evaluation. Thus, their ability to elicit significant action into the late phase might be attributed to the inhibition of the release of prostaglandins.

Table 3 Carrageenan induced paw oedema and cotton pellet induced granuloma in rats

Compound	Swelling thickness in mm (% inhibition)							Cotton pellet induced granuloma
	0 h	1 h	2 h	3 h	4 h	5 h	6 h	Wt. of granulation (mg) \pm S.D
Control	3.23 \pm 0.26	8.02 \pm 0.63	8.68 \pm 0.67	8.80 \pm 0.64	8.72 \pm 0.68	8.48 \pm 0.63	8.23 \pm 0.68	90.72 \pm 6.28
Indo	3.02 \pm 0.21	3.59 \pm 0.23 ^a (55.24)	3.60 \pm 0.27 ^a (58.52)	3.30 \pm 0.22 ^a (62.50)	3.21 \pm 0.25 ^a (63.19)	3.09 \pm 0.28 ^a (63.56)	3.26 \pm 0.19 ^a (60.39)	51.68 \pm 3.83 ^a
Celecoxib	3.12 \pm 0.20	3.75 \pm 0.30 ^a (53.24)	3.81 \pm 0.35 ^a (56.11)	3.35 \pm 0.31 ^a (61.93)	3.23 \pm 0.29 ^a (62.96)	3.20 \pm 0.22 ^a (62.26)	3.19 \pm 0.30 ^a (61.24)	53.24 \pm 3.38 ^a
3c	3.19 \pm 0.29	5.04 \pm 0.45 ^{abc} (37.16)	4.84 \pm 0.44 ^{abc} (44.24)	3.93 \pm 0.36 ^{ab} (55.34)	3.51 \pm 0.32 ^a (59.75)	3.32 \pm 0.25 ^a (60.85)	3.29 \pm 0.29 ^a (60.02)	54.78 \pm 4.04 ^a
3d	3.07 \pm 0.23	4.91 \pm 0.45 ^{abc} (38.78)	4.68 \pm 0.41 ^{abc} (46.08)	3.74 \pm 0.32 ^a (57.50)	3.53 \pm 0.29 ^a (59.52)	3.31 \pm 0.23 ^a (60.97)	3.28 \pm 0.31 ^a (60.14)	54.19 \pm 3.67 ^a
3e	3.19 \pm 0.27	4.95 \pm 0.42 ^{abc} (38.28)	4.76 \pm 0.44 ^{abc} (45.16)	3.58 \pm 0.31 ^a (59.32)	3.45 \pm 0.29 ^a (60.43)	3.26 \pm 0.28 ^a (61.56)	3.26 \pm 0.24 ^a (60.39)	55.24 \pm 4.05 ^a
4c	3.24 \pm 0.20	5.20 \pm 0.50 ^{abc} (35.16)	4.97 \pm 0.47 ^{abc} (42.74)	3.94 \pm 0.35 ^{ab} (55.23)	3.56 \pm 0.31 ^a (59.17)	3.46 \pm 0.20 ^a (59.20)	3.43 \pm 0.33 ^a (58.32)	55.82 \pm 3.92 ^a
4d	3.31 \pm 0.28	5.31 \pm 0.46 ^{abc} (33.79)	5.20 \pm 0.48 ^{abc} (40.10)	4.07 \pm 0.36 ^{abc} (53.75)	3.75 \pm 0.34 ^a (56.99)	3.57 \pm 0.31 ^a (57.90)	3.59 \pm 0.33 ^a (56.38)	55.82 \pm 4.17 ^a
4e	3.15 \pm 0.22	5.07 \pm 0.43 ^{abc} (36.78)	4.79 \pm 0.37 ^{abc} (44.81)	3.92 \pm 0.33 ^{ab} (55.45)	3.63 \pm 0.31 ^a (58.37)	3.52 \pm 0.30 ^a (58.49)	3.36 \pm 0.32 ^a (59.17)	55.93 \pm 4.11 ^a
5d	3.28 \pm 0.22	5.74 \pm 0.52 ^{abc} (28.43)	6.05 \pm 0.58 ^{abc} (30.30)	5.38 \pm 0.44 ^{abc} (38.86)	4.98 \pm 0.36 ^{abc} (42.89)	4.80 \pm 0.39 ^{abc} (43.40)	4.71 \pm 0.45 ^{abc} (42.77)	nt
5e	3.45 \pm 0.28	6.01 \pm 0.41 ^{abc} (25.06)	6.18 \pm 0.40 ^{abc} (28.80)	6.18 \pm 0.55 ^{abc} (29.77)	5.82 \pm 0.52 ^{abc} (33.26)	5.25 \pm 0.49 ^{abc} (38.09)	5.29 \pm 0.43 ^{abc} (35.72)	nt

Values are expressed as the mean \pm S.D (n = 6).

a: $p < 0.05$ vs. Control; **b:** $p < 0.05$ vs. Indo; **c:** $p < 0.05$ vs. Celecoxib

Control: 0.3% sodium CMC solution in distilled water (10 ml kg⁻¹, *p.o.*);

All compounds and standard drugs were administered at a dose of 0.0279 mmol kg⁻¹, *p.o.* in 0.3% sodium CMC solution

nt: Not tested

2.2.4. Cotton pellet induced granuloma

Cotton pellet induced granuloma formation is a typical feature of an established inflammatory reaction, which has been extensively used to assess the transudative and proliferative components of chronic inflammation. The fluid adsorbed by the pellet significantly influences the wet weight of the granuloma, whereas the dry weight correlates well with the amount of granulomatous tissue formed [43]. In this study, the compounds **3c-3e**, **4c-4e** and the standard drugs decreased both the wet and dry weight of the cotton pellets as compared to the control group (**Table 3**). The results reflected their efficacy to reduce the elevated level of fibroblasts and synthesis of collagen with mucopolysaccharide, which are natural proliferative events of granulomatous tissue formation.

2.2.5. Freund's adjuvant induced arthritis

In the investigation of Freund's complete adjuvant (FCA) induced arthritis, it was observed that the paw swelling and thickness which developed over a period of 24 h post adjuvant injection, subsided slightly for next 5-8 days and then increased when arthritis appeared. The treatment which was initiated 14 days post adjuvant induction suppressed the subsequent increase in swelling of the injected foot, which occurred, with the appearance of polyarthritis. The determination of foot thickness of the rats was used in evaluating anti-inflammatory activity and therapeutic effects of the treatment. It was observed that the compounds **3c-3e**, **4c-4e** and the standard drugs exhibited anti-arthritic effect evidenced by a significant progressive reduction in paw swelling compared with arthritic control animals ($p < 0.05$) for 21 days (**Table 4**). It is evident from the reported literature that FCA induces arthritis, where both T cell and B cell activation play a major role. Cytokines of Th1 (IFN γ secreting) and Th2 cells (IL-4 secreting) are generated wherein Th1 profile predominates at the onset of disease [44]. Thus, the ability of the compounds to reduce oedema formation may be imputed to their inhibitory effects on cytokines in addition to prostaglandins.

2.2.6. Ulcerogenic studies

Compounds exhibiting prominent *in-vivo* anti-inflammatory profiles were further evaluated for their ulcerogenic liability. The results depicted in **Table 4** revealed that the compounds **3c-3e**, **4c-4e** exhibited a low ulcer index (UI). Also, no significant difference was observed in UI as compared to standard celecoxib. Histological study of the gastric mucosa revealed that compounds **3d**, **3e** and **4c** evoked a minimal gastric insult as compared to indomethacin which on prolonged administration caused severe detachment of surface epithelium, resulting in the formation of gastric lesions (**Fig. 2**).

2.2.7. Lipid Peroxidation studies

The lipid peroxidation profile of the compounds **3c-3e** and **4c-4e** was assessed to validate the ulcerogenic activity (**Table 4**) results since compounds eliciting less ulcerogenic liability also exhibited reduced malondialdehyde (MDA) content, a by-product of lipid peroxidation [45]. Apart from eliciting minimal ulcerogenic liability, the compounds also exhibited a marked reduction in lipid peroxidation. Indomethacin elicited the highest lipid peroxidation, 8.38 ± 0.57 nmol MDA 100 mg^{-1} tissue, whereas the control group exhibited a lipid peroxidation of 4.24 ± 0.34 nmol MDA 100 mg^{-1} tissue under similar experimental conditions. These results further support the protective effect of the compounds on the inhibition of lipid peroxidation in the gastric mucosal wall.

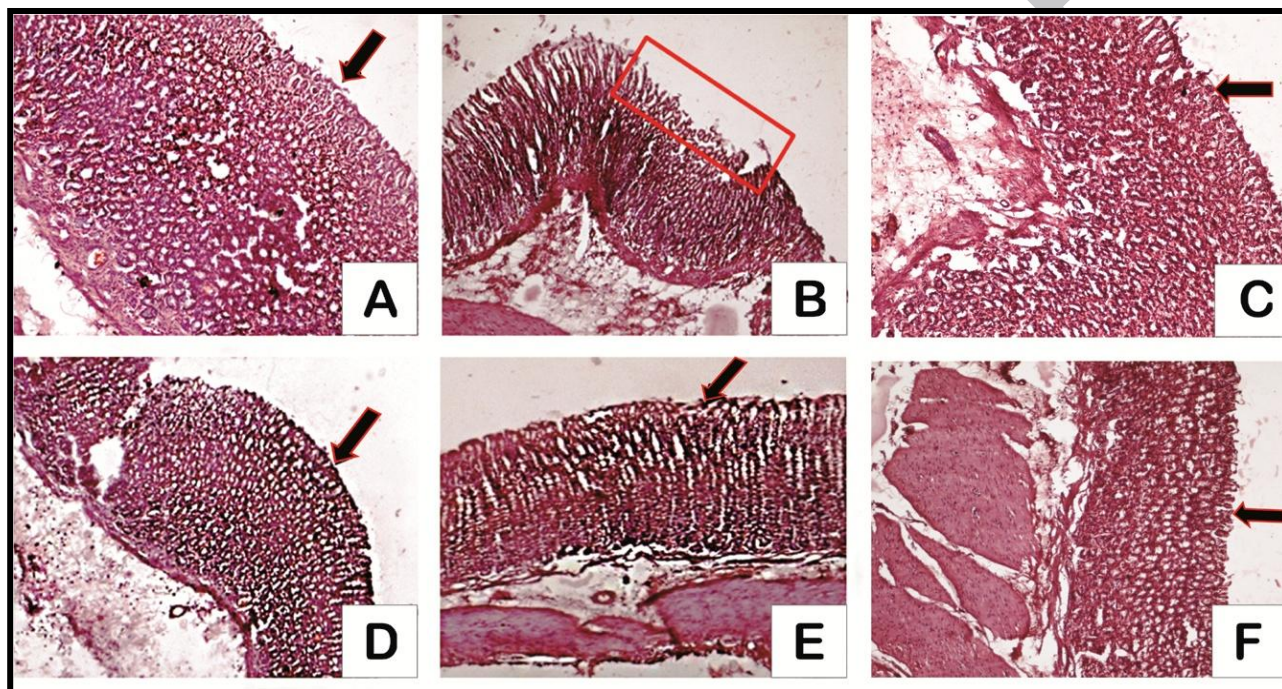


Fig. 2. Photomicrographs (10x magnification) of [A] Control group; [B]: Indomethacin; [C]: Celecoxib; [D]: Compound **3d** [E]: Compound **3e** [F]: Compound **4c** treated groups in rat stomach tissues (hematoxylin and eosin staining). [Indications: Red box indicates severe detachment of surface epithelium, resulting in the formation of gastric lesions, Arrows indicates the normal stomach architecture with little or no ulcer formation].

2.2.8 Assessment of hepatic and renal functions

Compounds **3c-3e**, **4c-4e** were evaluated for hepatic and renal toxic liabilities through their effects on various serum biomarkers for liver and renal function parameters (serum enzymes, total protein, and total albumin). The outcome of the estimation of different biochemical parameters (**Table 5**) confirmed their relative safety compared with the standard drugs for prolonged use. This was further established by the histological studies of both the organs (**Fig. 3** and **Fig. 4**), which exhibited very little or no inflammatory cell infiltrate, oedema, epithelial cell loss, necrosis or degeneration in the hepatocytes and nephrons, respectively, compared to the indomethacin-treated group.

Table 4 Adjuvant-induced arthritis, ulcer index and lipid peroxidation assay

Compound	Paw thickness (mm) mean \pm S.D (% inhibition)							Ulcer Index \pm S.D	nmol for MDA content \pm S.D 100 mg ⁻¹ tissue
	Day 03	Day 06	Day 09	Day 12	Day 15	Day 18	Day 21		
Control	7.92 \pm 0.58	8.10 \pm 0.62	8.32 \pm 0.60	8.38 \pm 0.64	8.44 \pm 0.60	8.51 \pm 0.63	8.56 \pm 0.61	0	4.24 \pm 0.34
Indo	5.53 \pm 0.40 ^a (30.18)	4.96 \pm 0.42 ^a (38.77)	4.62 \pm 0.42 ^a (44.47)	4.47 \pm 0.41 ^a (46.66)	3.96 \pm 0.35 ^a (53.08)	3.54 \pm 0.33 ^a (58.40)	3.45 \pm 0.31 ^a (59.70)	55 \pm 3.8	8.38 \pm 0.57 ^a
Celecoxib	5.44 \pm 0.46 ^a (31.31)	5.11 \pm 0.43 ^a (36.91)	4.96 \pm 0.34 ^a (40.38)	4.76 \pm 0.41 ^a (43.20)	4.25 \pm 0.40 ^a (49.64)	3.99 \pm 0.35 ^a (53.11)	3.77 \pm 0.32 ^a (55.96)	26 \pm 1.9	6.82 \pm 0.54 ^{ab}
3c	5.67 \pm 0.47 ^a (28.41)	5.53 \pm 0.52 ^{ab} (31.73)	5.09 \pm 0.44 ^a (38.82)	4.90 \pm 0.42 ^a (41.53)	4.57 \pm 0.43 ^a (45.85)	4.41 \pm 0.40 ^{ab} (48.18)	4.14 \pm 0.38 ^a (51.64)	22 \pm 1.8	4.67 \pm 0.35 ^{abc}
3d	5.77 \pm 0.55 ^a (27.15)	5.64 \pm 0.43 ^a (30.37)	5.23 \pm 0.46 ^a (37.14)	4.94 \pm 0.41 ^a (41.05)	4.48 \pm 0.37 ^a (46.92)	4.33 \pm 0.41 ^{ab} (49.12)	4.09 \pm 0.36 ^a (52.22)	20 \pm 1.1	4.18 \pm 0.37 ^{abc}
3e	5.52 \pm 0.42 ^a (30.30)	5.35 \pm 0.47 ^a (33.95)	5.05 \pm 0.45 ^a (39.30)	4.68 \pm 0.41 ^a (44.15)	4.28 \pm 0.39 ^a (49.29)	3.96 \pm 0.36 ^a (53.47)	3.83 \pm 0.35 ^a (55.26)	24 \pm 2.0	4.31 \pm 0.39 ^{abc}
4c	5.74 \pm 0.48 ^a (27.53)	5.66 \pm 0.43 ^{ab} (30.12)	5.40 \pm 0.31 ^{ab} (35.10)	4.85 \pm 0.43 ^a (42.12)	4.70 \pm 0.40 ^{ab} (44.31)	4.39 \pm 0.38 ^{ab} (48.41)	4.12 \pm 0.28 ^a (51.87)	23 \pm 1.5	4.54 \pm 0.38 ^{abc}
4d	5.57 \pm 0.51 ^a (29.67)	5.44 \pm 0.41 ^a (32.84)	5.35 \pm 0.43 ^{ab} (35.70)	5.11 \pm 0.45 ^a (39.02)	4.83 \pm 0.47 ^{ab} (42.77)	4.45 \pm 0.42 ^{ab} (47.71)	4.20 \pm 0.37 ^{ab} (50.93)	24 \pm 2.2	4.83 \pm 0.33 ^{abc}
4e	5.68 \pm 0.54 ^a (28.28)	5.62 \pm 0.48 ^a (30.62)	5.30 \pm 0.50 ^a (36.30)	4.90 \pm 0.30 ^a (41.53)	4.72 \pm 0.42 ^{ab} (44.08)	4.47 \pm 0.41 ^{ab} (47.47)	4.18 \pm 0.28 ^{ab} (51.17)	22 \pm 1.3	5.02 \pm 0.41 ^{abc}

Values are expressed as the mean \pm S.D (n = 6).

a: p < 0.05 vs. Control; **b:** p < 0.05 vs. Indo 10; **c:** p < 0.05 vs. Celecoxib

Control: 0.3% sodium CMC solution in distilled water (10 ml kg⁻¹, *p.o.*);

All compounds and standard drugs were administered at a dose of 0.0279 mmol kg⁻¹, *p.o.* in 0.3% sodium CMC solution.

Table 5 Effect of compounds on hepatic and renal function parameters as evaluated on 21st day after treatment

Compound	SGOT (U mL ⁻¹)	SGPT (U mL ⁻¹)	ALP (U mL ⁻¹)	Total protein (g dL ⁻¹)	Total albumin (g dL ⁻¹)	CR (mg dL ⁻¹)	BUN (mg dL ⁻¹)
Control	90.87 \pm 6.38	31.36 \pm 2.20	18.12 \pm 0.96	1.91 \pm 0.13	1.62 \pm 0.09	0.58 \pm 0.039	21.88 \pm 1.42
Indo 10	118.68 \pm 8.23 ^a	51.34 \pm 3.91 ^a	27.18 \pm 1.53 ^a	2.32 \pm 0.15 ^a	2.48 \pm 0.17 ^a	1.91 \pm 0.12 ^a	63.17 \pm 1.54 ^a

Celecoxib	113.56 ± 8.38 ^a	48.33 ± 3.65 ^a	25.83 ± 1.68 ^a	2.21 ± 0.15 ^a	2.30 ± 0.14 ^a	1.32 ± 0.07 ^{ab}	61.38 ± 1.49 ^a
3c	97.89 ± 7.68 ^{bc}	38.11 ± 3.09 ^{abc}	20.67 ± 1.23 ^{bc}	2.02 ± 0.14 ^b	1.82 ± 0.14 ^{bc}	0.91 ± 0.05 ^{abc}	42.78 ± 1.32 ^{abc}
3d	98.77 ± 7.42 ^{bc}	41.34 ± 3.15 ^{abc}	21.34 ± 1.55 ^{abc}	2.03 ± 0.17 ^b	1.92 ± 0.15 ^{abc}	1.17 ± 0.07 ^{abc}	45.78 ± 1.36 ^{abc}
3e	98.12 ± 7.18 ^{bc}	38.88 ± 2.94 ^{abc}	20.97 ± 1.56 ^{abc}	1.98 ± 0.13 ^b	1.88 ± 0.16 ^{bc}	1.04 ± 0.07 ^{abc}	45.17 ± 1.36 ^{abc}
4c	96.91 ± 6.98 ^{bc}	40.20 ± 3.34 ^{abc}	21.09 ± 1.62 ^{abc}	2.00 ± 0.12 ^b	1.96 ± 0.17 ^{abc}	0.95 ± 0.06 ^{abc}	47.24 ± 1.34 ^{abc}
4d	97.23 ± 7.07 ^{bc}	39.78 ± 3.11 ^{abc}	22.11 ± 1.66 ^{abc}	1.97 ± 0.16 ^b	1.87 ± 0.18 ^{bc}	1.08 ± 0.05 ^{abc}	48.71 ± 1.41 ^{abc}
4e	97.88 ± 7.41 ^{bc}	41.97 ± 3.57 ^{abc}	22.54 ± 1.60 ^{abc}	2.00 ± 0.18 ^b	1.95 ± 0.17 ^{abc}	1.20 ± 0.08 ^{abc}	49.83 ± 1.40 ^{abc}

SGOT: Serum Glutamic Oxaloacetic Transaminase;

SGPT: Serum Glutamic Pyruvic Transaminase;

ALP: Alkaline Phosphatase; CR: Creatinine;

BUN: Blood Urea Nitrogen

Values are expressed as the mean ± S.D (n = 6).

a: p < 0.05 vs. Control; **b:** p < 0.05 vs. Indo 10; **c:** p < 0.05 vs. Celecoxib

Control: 0.3% sodium CMC solution in distilled water (10 ml kg⁻¹, *p.o.*);

All compounds and standard drugs were administered at a dose of 0.0279 mmol kg⁻¹, *p.o.* in 0.3% sodium CMC solution.

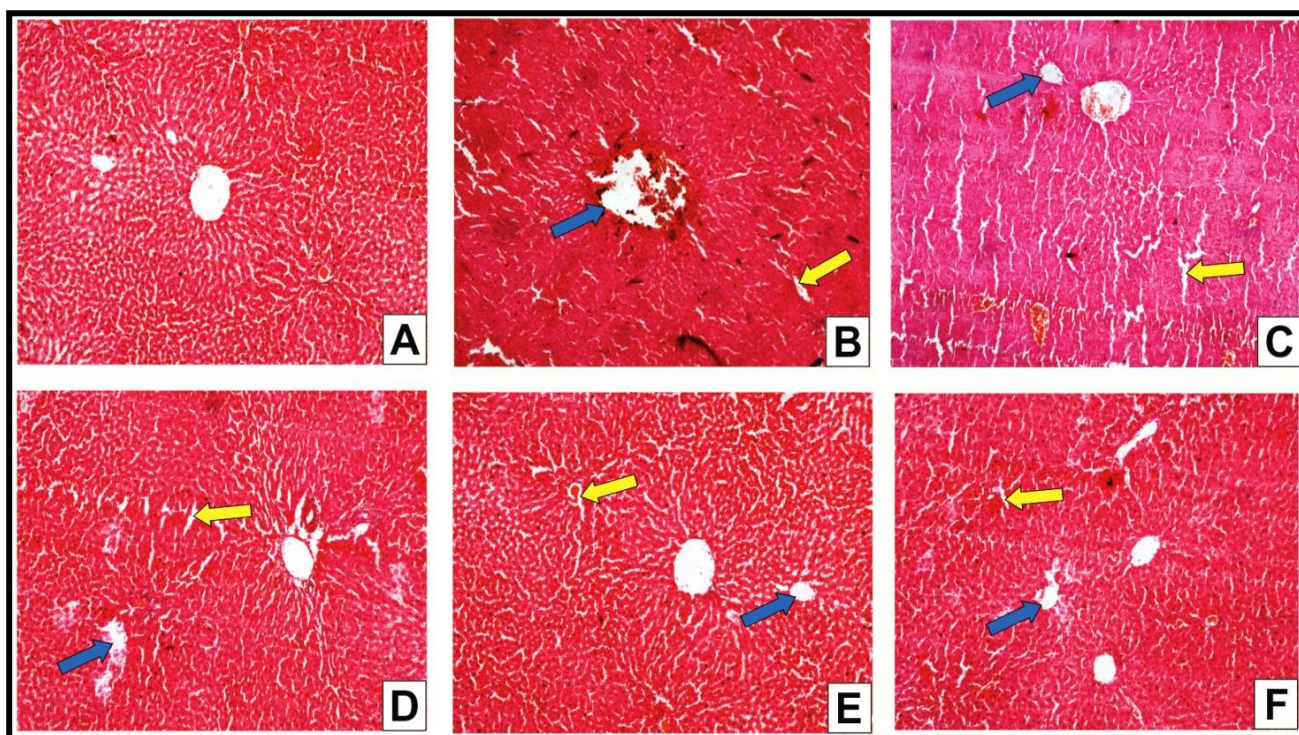


Fig. 3. Photomicrographs (10x magnification) of [A] Control; [B] Indomethacin; [C] Celecoxib [D] Compound **3d** [E]: Compound **3e** [F]: Compound **4c** treated groups in rat liver tissues (hematoxylin and eosin staining). Blue arrows indicate fibrosis and fatty degeneration. Yellow arrows indicate dilated sinusoids.

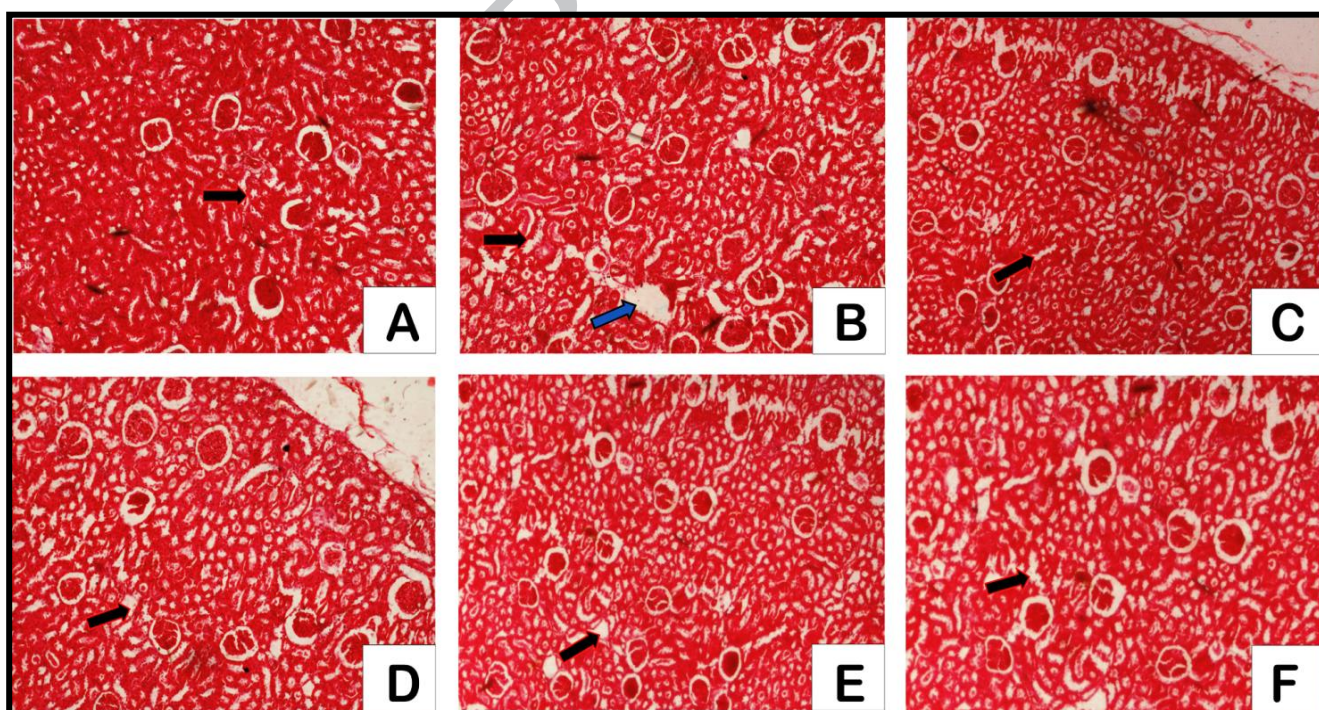


Fig. 4. Photomicrographs (10x magnification) of [A] Control; [B] Indomethacin; [C] Celecoxib [D] Compound **3d** [E]: Compound **3e** [F]: Compound **4c** treated groups in rat kidney tissues (hematoxylin and eosin staining). The black arrow indicates atrophy of renal tubule. Blue arrow indicates mild tubular dilation of renal cortex and medulla.

2.2.9. *In vitro* COX inhibition assay & enzyme kinetics studies

Compounds **3c-3e** and **4c-4e** were evaluated *in vitro* against COX-1 and COX-2 to determine the IC₅₀ values and ascertain their specificity. Amongst the estimated compounds, the 1,2,4-oxadiazole derivative bearing a 4-nitrophenyl substitution (**3e**) and its 4-chlorophenyl counterpart (**3d**) were the most potent COX-2 inhibitors with IC₅₀ values of 0.60 μM and 0.65 μM, respectively. As evidenced by the IC₅₀ and selectivity index data in **Table 6**, unlike indomethacin, a non-selective COX inhibitor (SI index = 1.03), these compounds displayed higher selectivity towards the inhibition of COX-2 over COX-1 which confirmed their selective COX-2 inhibitory potential. It explains their improved gastric tolerability on prolonged use.

Furthermore, substrate dependent kinetic parameters were determined to characterise the mechanism of inhibition of COX-2 isoform by compounds **3c-3e** and **4c-4e**. The kinetic parameters of the present study were determined based on Michaelis-Menten equation followed by a Lineweaver-Burk double reciprocal analysis of dataset regarding 1/V_{max} Vs 1/[S] plot. The Lineweaver-Burk plot analysis of the compounds revealed them as competitive inhibitors. As shown in **Fig. 5**, the 1/V_{max} (y-intercept) values for compounds **3c-3e** and **4c-4e** are as same as that of no inhibitor, confirming their competitive inhibitory nature for COX-2 on its substrate arachidonic acid.

Table 6 COX inhibitory activity and selectivity index (COX-1/COX-2) of selected compounds

Compound	IC ₅₀ (μM) ^a		COX-2 Selectivity index ^b	Type of Inhibition for COX-2	COX-2 K _i (μM)
	COX-1	COX-2			
3c	60.54 ± 4.38 ^g	0.77 ± 0.023 ^g	78.62	competitive	0.65
3d	64.53 ± 4.12 ^g	0.65 ± 0.028 ^g	99.28	competitive	0.63
3e	62.44 ± 3.77 ^g	0.60 ± 0.025 ^g	104.07	competitive	0.50
4c	60.06 ± 3.89 ^g	0.90 ± 0.037 ^g	66.73	competitive	0.77
4d	62.19 ± 4.42 ^g	1.11 ± 0.075 ^g	56.03	competitive	0.96
4e	63.17 ± 3.82 ^g	1.01 ± 0.068 ^g	62.54	competitive	0.88
Indomethacin	3.79 ± 0.12	3.67 ± 0.15	1.03	nt	nt
Celecoxib	58.29 ± 2.13 ^g	0.54 ± 0.022 ^g	107.94	competitive	0.49

IC₅₀ values are expressed as the mean ± S.D (n = 2); nt= Not tested

^aValues acquired using an ovine COX assay kit (Catalog No. 760111, Cayman Chemical Inc., Ann Arbor, MI). Experiments were carried out in duplicate and had <10% error.

^bSelectivity for COX-2 defined as IC₅₀ (COX-1)/IC₅₀ (COX-2)

^g: p < 0.05 vs. Indomethacin

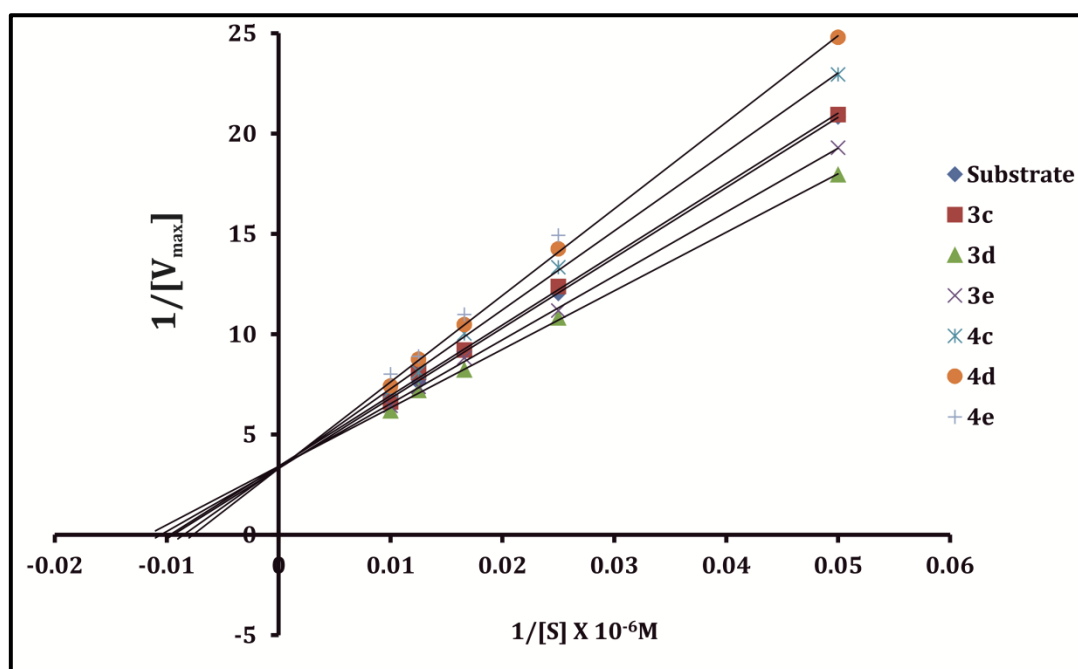


Fig. 5. Lineweaver–Burk plot of *in vitro* COX-2 inhibition by compounds **3c-3e** and **4c-4e**

2.2.10. Evaluation of cardiotoxic liability

Based on the outcome of the *in vitro* COX inhibition assay study, the most potent compound from the 1,3,4-oxadiazole series (**3e**) and 1,3,4-thiadiazole series (**4c**) was selected and evaluated for their cardiotoxic liability in myocardial infarcted rats. Serum levels of biomarkers such as cardiac troponin I (cTnI) and Creatine kinase-MB (CK-MB) are useful in establishing the diagnosis of myocardial infarction [46]. It has been reported that isoproterenol (ISO) causes myocardial infarction (MI) by increasing the levels of cTnI and CK-MB in the serum of the animals [47, 48] and is a well-developed non-invasive animal model of MI [49]. The advantage of this model over surgical method lies in its simplicity, non-invasive technique thus no chance of contracting post-surgical infections and a low mortality rate. The pattern of ischemic necrosis ISO-induced MI is analogous to humans because it produces maximum necrosis in the ventricular subendocardial region and inter-ventricular septum [50].

Alteration in serum levels of cardiac injury biomarkers (cTnI and CK-MB) in both normal and ISO-induced MI in rats are presented in **Table 7 & 8**. Administration of ISO resulted in a significant increase ($p < 0.05$) in serum levels of both cTnI and CK-MB in myocardial infarcted rats as compared to the normal control group. In the myocardial infarcted rats, an initial spike was observed in the serum levels of cTnI and CK-MB on day 3 and day 4 which subsided on day 7 and eventually returned to their basal levels on day 11 maintaining the same till day 19. Based on this outcome, we can reasonably conclude that the treatment of animals within the MI group with

standard celecoxib and compounds **3e** and **4c** did not aggravate the existing condition. The results thus elicit the absence of cardiotoxic liability of the compounds **3e** and **4c**.

Table 7 Effects of celecoxib, **3e** and **4c** on the levels of serum cardiac troponin-I on ISO induced myocardial infarcted rats.

Treatment	cTnI levels (ng/ml) in Mean \pm SD					
	Day 0	Day 3	Day 4	Day 7	Day 11	Day 19
Normal Control	0.58 \pm 0.044	0.55 \pm 0.040	0.57 \pm 0.041	0.57 \pm 0.045	0.58 \pm 0.045	0.57 \pm 0.043
ISO Control	0.67 \pm 0.050	2.82 \pm 0.198 ^a	1.90 \pm 0.138 ^a	0.92 \pm 0.037 ^a	0.70 \pm 0.029	0.69 \pm 0.032
ISO+Celecoxib	0.58 \pm 0.030	2.88 \pm 0.192 ^a	1.78 \pm 0.122 ^a	0.84 \pm 0.030 ^a	0.69 \pm 0.033	0.68 \pm 0.028
ISO+ 3e	0.56 \pm 0.022	2.90 \pm 0.195 ^a	1.82 \pm 0.127 ^a	0.80 \pm 0.028 ^a	0.68 \pm 0.030	0.58 \pm 0.028
ISO+ 4c	0.54 \pm 0.038	2.92 \pm 0.191 ^a	1.77 \pm 0.134 ^a	0.85 \pm 0.033 ^a	0.62 \pm 0.027	0.60 \pm 0.022

Values are expressed as the mean \pm S.D (n = 6).

a: p < 0.05 vs. Control.

Normal Control: 0.3% sodium CMC solution in distilled water (10 ml kg⁻¹, *p.o.*);

ISO Control: Isoproterenol (100 mg kg⁻¹, *s.c.*).

Compounds (Celecoxib, **3e** and **4c**) were administered at a dose of 0.0279 mmol kg⁻¹, *p.o.* in 0.3% sodium CMC

Table 8 Effects of celecoxib, **3e** and **4c** on the levels of serum creatine kinase-MB (CK-MB) on ISO induced myocardial infarcted rats

Treatment	CK-MB levels (ng/ml) in Mean \pm SD					
	Day 0	Day 3	Day 4	Day 7	Day 11	Day 19
Normal Control	14.24 \pm 0.92	14.29 \pm 0.99	14.27 \pm 0.98	14.25 \pm 0.95	14.25 \pm 0.97	14.26 \pm 0.93
ISO Control	15.57 \pm 1.12	102.30 \pm 7.34 ^a	70.26 \pm 4.42 ^a	32.68 \pm 1.98 ^a	17.86 \pm 1.26	17.22 \pm 1.21
ISO+Celecoxib	15.42 \pm 1.17	100.78 \pm 7.88 ^a	72.32 \pm 5.04 ^a	35.15 \pm 2.04 ^a	17.63 \pm 1.11	17.17 \pm 1.19
ISO+ 3e	14.84 \pm 1.12	98.69 \pm 6.79 ^a	69.28 \pm 4.42 ^a	31.33 \pm 2.16 ^a	15.29 \pm 1.23	15.02 \pm 1.30
ISO+ 4c	14.68 \pm 1.20	100.72 \pm 7.42 ^a	69.43 \pm 4.88 ^a	33.57 \pm 2.08 ^a	16.75 \pm 1.33	16.13 \pm 1.37

Values are expressed as the mean \pm S.D (n = 6).

a: p < 0.05 vs. Control.

Normal Control: 0.3% sodium CMC solution in distilled water (10 ml kg⁻¹, *p.o.*);

ISO Control: Isoproterenol (100 mg kg⁻¹, *s.c.*).

Compounds (Celecoxib, **3e** and **4c**) were administered at a dose of 0.0279 mmol kg⁻¹, *p.o.* in 0.3% sodium CMC

2.3. Computational Studies

2.3.1. Molecular docking studies

Molecular docking studies were performed using the GLIDE (Grid-Based Ligand Docking with Energetics) extra precision (XP) programme to gain insight into the possible mode of protein-ligand interaction at the COX-2 active site. Validation of docking experiment was performed by using the superposition tool in Schrödinger Maestro 10.5.014 with celecoxib as the co-crystallized ligand (PDB ID: 3LN1). The RMSD (root mean square deviation) value equal to 0.318 Å (See

Supplementary, **Fig. S25**) suggested that predicted and actual crystallographic conformation of celecoxib were within the acceptable limit of 2 Å [51]. It confirmed that the parameters set for Glide-XP docking mode were reliable in generating reproducible *in silico* binding mode for COX-2 inhibitors.

The potent compounds **3e** (IC₅₀: 0.60 μM) (GLIDE Score: -11.95); **3d** (IC₅₀: 0.65 μM) (GLIDE Score: -11.72) and **3c** (IC₅₀: 0.77 μM) (GLIDE Score: -10.82) exhibited a Y-shaped structure wherein the biphenyl rings stretched effectively to interact with the hydrophobic amino acid residues Ile 503, Arg 499, Ala 502, Val 509, Leu 338, Met 508, and Ala 513 (**Fig. 6a, 6b & 6c**). It facilitated in anchoring the molecules deep within the enzyme gorge of the COX-2 active site contributing to better complex stabilisation. The compound **3e** revealed that hydrogen bond interaction between the oxygen atom of the 1,3,4-oxadiazole ring and His 75 was (2.43 Å). Another hydrogen bond was observed between the -NH linker of **3e** and Gln 178 (2.47 Å). For compound **3d**, hydrogen bonding (1.94 Å) was found between Ser 339 and the -NH linker group. Similarly, for compound **3e**, hydrogen bonding interaction (1.94 Å) was observed between Ser 339 and the -NH linker group. The outcome of the docking exercise thus exemplified the consensual interaction of the docked ligand within the COX-2 active site.

Docking studies also helped to shed light on the importance of the -NH linker. The presence of an additional -NH linker bonded to five member oxadiazole/thiadiazole on one end and substituted aryl group on the other provided additional leverage to the aryl appendage further improves the overall flexibility of the molecule. The presence of a properly spaced protonable amino group coupled with the aromatic and heteroaromatic residues facilitated additional interaction with the amino acid within the COX-2 active site (**Fig. 6a, 6b & 6c**). This might explain the significant improvement towards the COX-2 inhibition of the potential compounds.

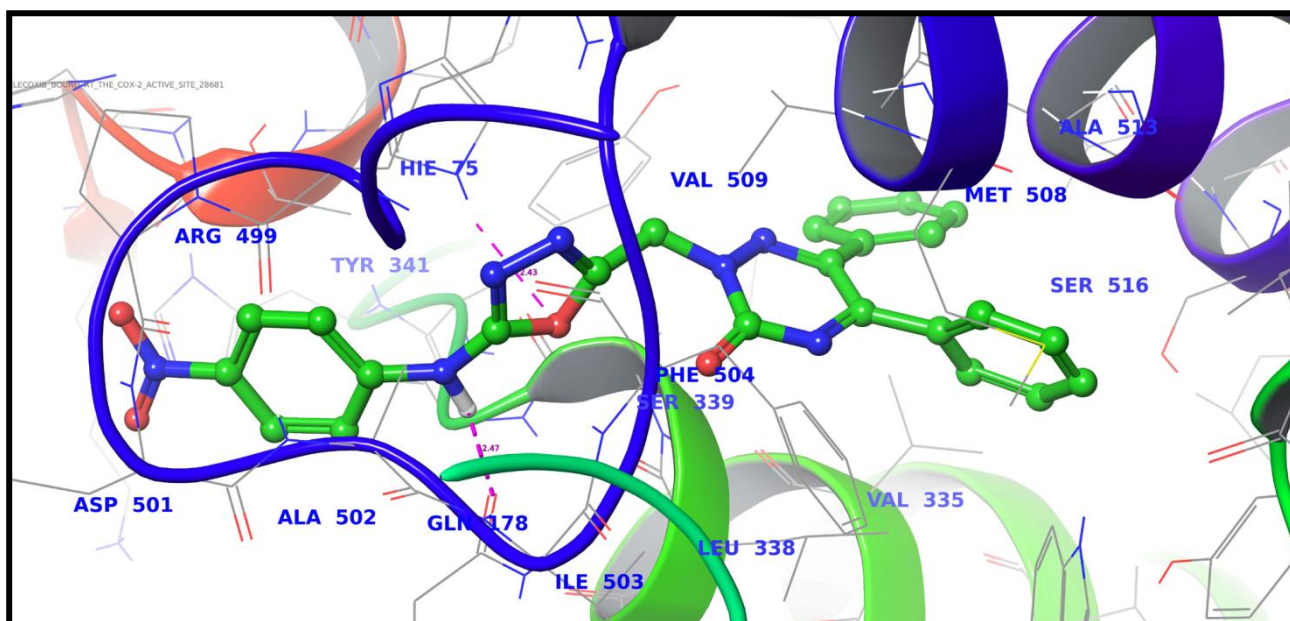


Fig.6a. 3D view of the docking study of the minimum energy structure of the complex of **3e** docked in COX-2 (PDB: 3LN1).

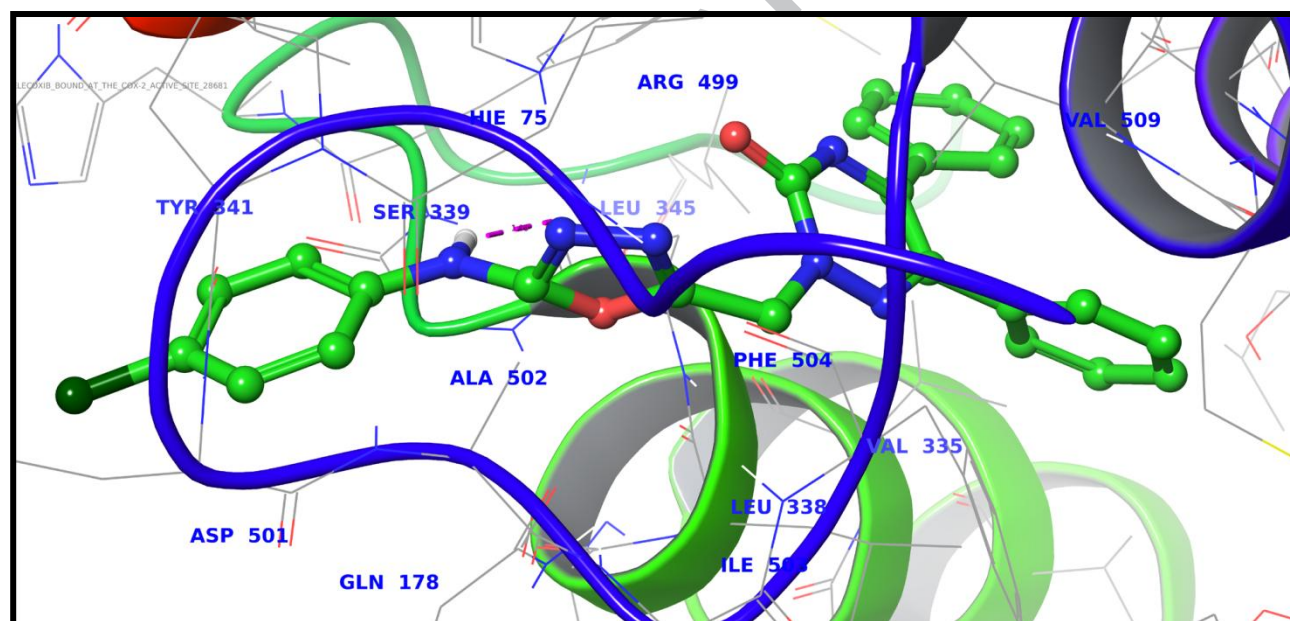


Fig.6b. 3D view of the docking study of the minimum energy structure of the complex of **3d** docked in COX-2 (PDB: 3LN1).

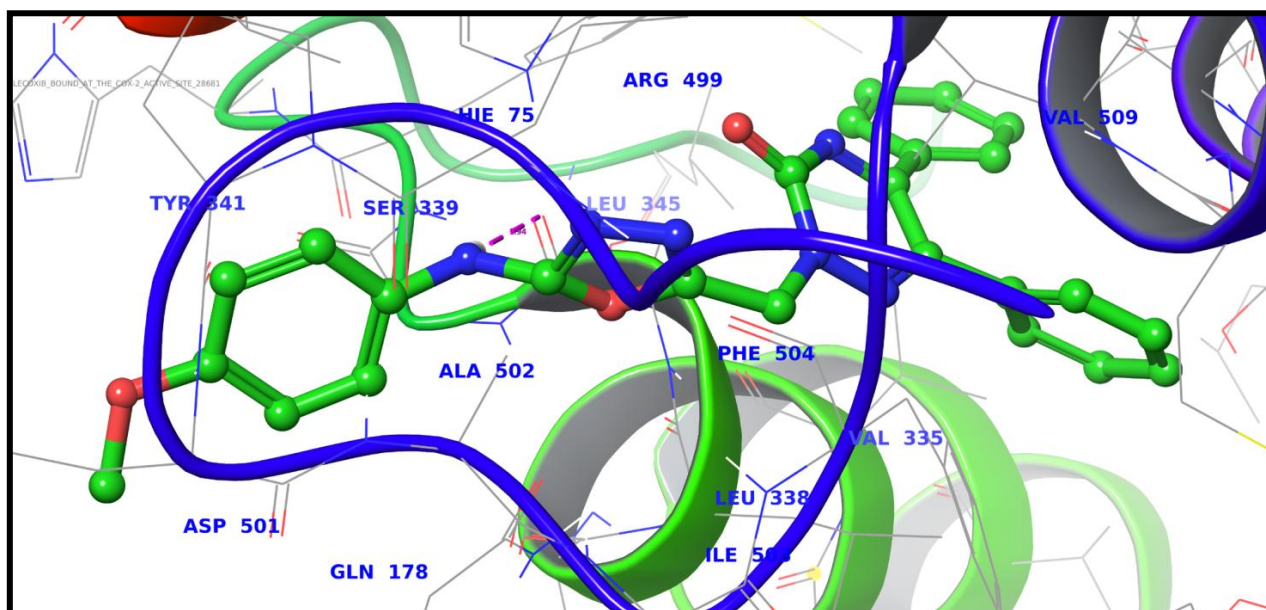


Fig.6c. 3D view of the docking study of the minimum energy structure of the complex of **3c** docked in COX-2 (PDB: 3LN1).

It was notable that the compounds (**5a-5e**) failed to dock into the COX-2 active site even after the docking parameters were relaxed to an extent. Further investigation into this phenomenon revealed that the peculiar L-shaped spatial arrangement of their minimum energy conformer (See Supplementary, **Fig. S26**) compounded with the absence of -NH linker increased their overall rigidity. It also restricted their entry into the COX-2 active site and subsequent interaction with the active amino acids. The outcome of the docking exercise thus explains the vitiated activity of compounds **5d** and **5e** as evidenced in the carrageenan induced rat paw oedema model. From this, one infer that not merely the presence of a particular pharmacophoric group but the rigid three-dimensional arrangement of its minimum energy conformer seem to get further aggravated by the absence of the -NH linker coupled with the aromatic planar moiety as observed in the case of compounds **5a-5e** was responsible for their diminished anti-inflammatory effect.

2.3.2. Molecular Dynamic (MD) simulations

A 20 nsec MD simulation of the solvated energy minimised docked complex of compound **3d** (also referred as 'ligand'), and COX-2 (PDB Id: 3LN1) was performed post-docking studies for the assessment of predicted binding mode. The overall stability of the system was evaluated by RMSD (Root Mean Square Deviation) and RMSF (Root Mean Square Fluctuation) calculations. RMSD values confirmed that all frames of the complex were in trajectory throughout the experiment when the atom of a particular frame was compared with the reference frame. The RMSD plot indicated that the protein backbone was stable through the phase of MD simulation and attained the equilibrium within 1.2 nsec with an average fluctuation of 1 Å (**Fig. 7**).

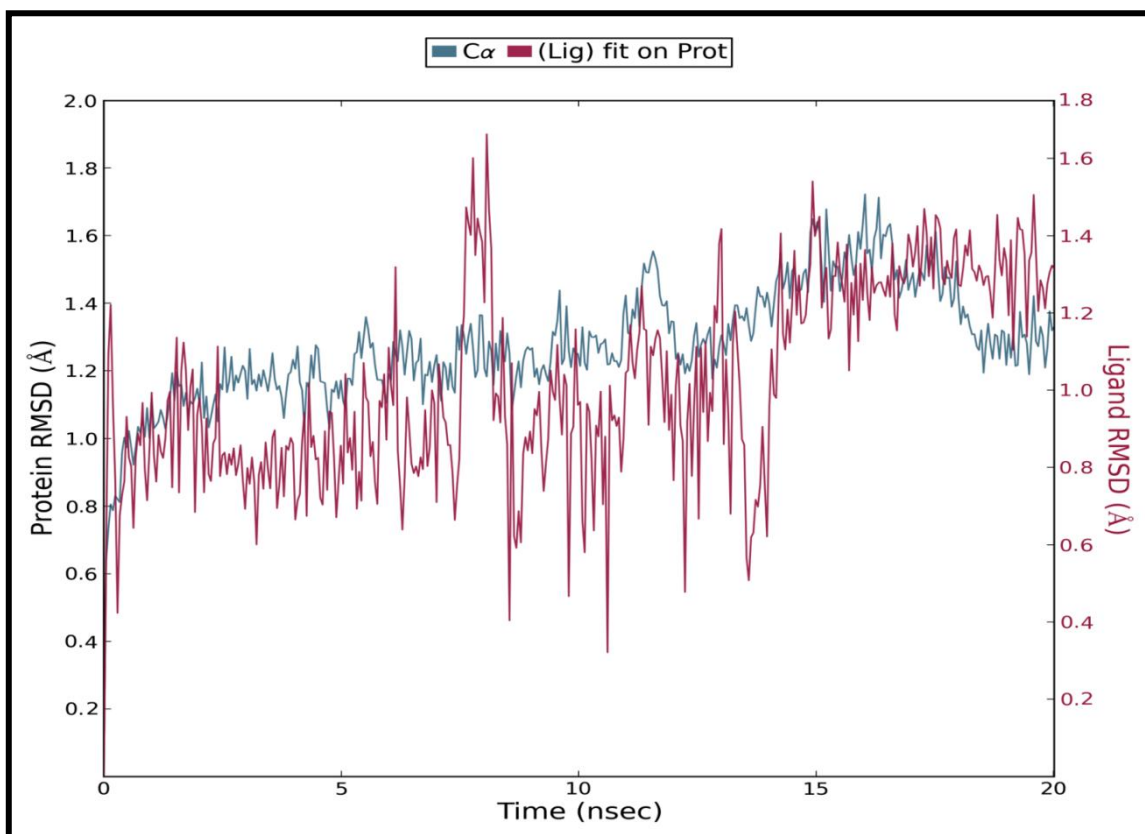


Fig. 7. Protein RMSD (Left Y-Axis) and ligand RMSD (Right Y-Axis) values in Å with time in nsec (X-Axis).

To further warrant the structural stability of each segment of the protein and compound **3e**, the protein RMSF and ligand RMSF were calculated, respectively. An RMSF value below 3 Å confirmed the absence of overall local changes along the protein chain and ligand atom position along the complete phase of the dynamic simulation run. A graphical examination of **Fig. 8** confirmed the binding of compound **3e** with the active amino acid residues in the COX-2 site. The snapshot revealed that the compound **3e** efficiently interacted through water bridges to form H-bond with critical polar amino acid residues His 75 and Tyr 341. Besides, it also interacted with other essential amino acids such as Arg 106, Leu 338, Val 335 and Ala 513 surrounding the COX-2 pocket through hydrophobic interactions. Protein interactions with compound **3e** were analysed and calculated as interaction fraction throughout the molecular dynamics simulation (**Fig. 9**). The stacked bar charts were normalised over the course of the trajectory: for example, fraction interaction value of 0.8 suggests that interaction was maintained through 80% of the total simulation time. It facilitated in evaluating the role of each of the particular bonds with the amino acid residues accountable for the overall stabilisation of the protein-ligand complex.

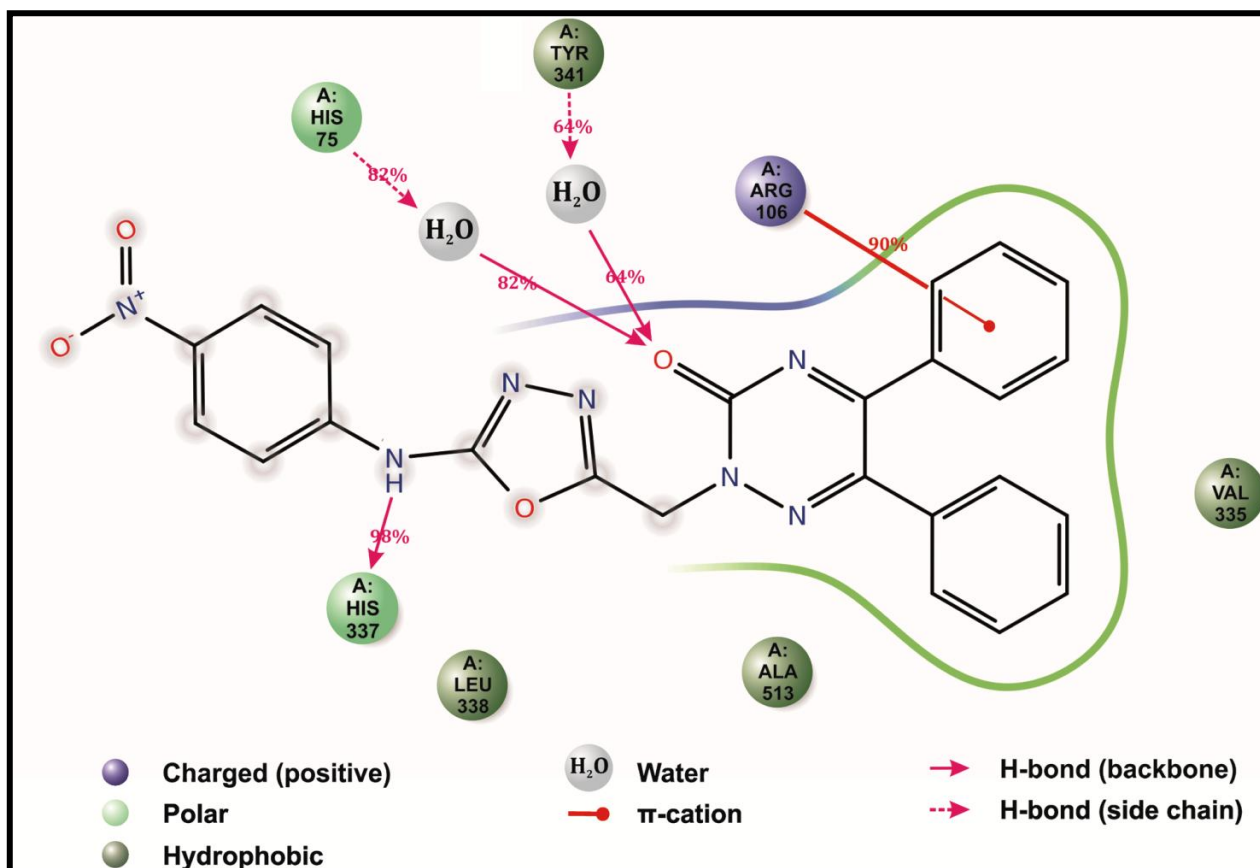


Fig. 8. The detailed atomic interactions of ligand **3e** with the key amino acid residues at the COX-2 active site.

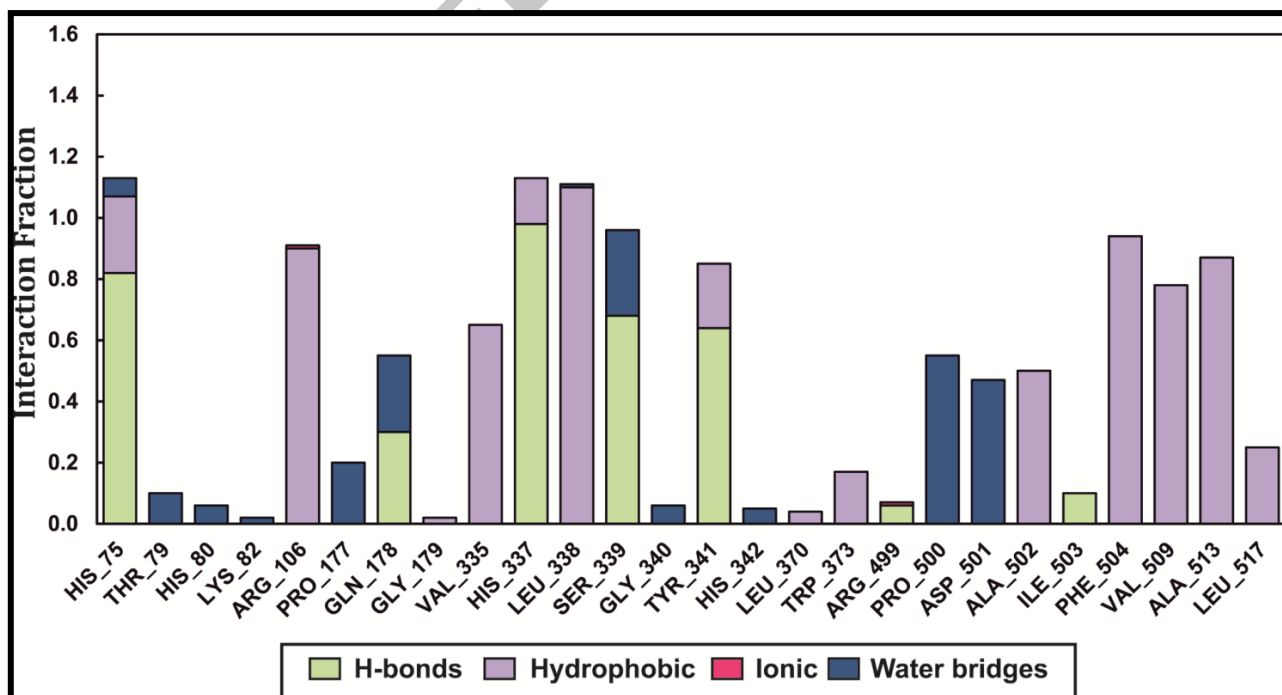


Fig. 9. Stacked bar charts of protein interactions with ligand **3e** as monitored throughout the MD simulation.

The MD simulations of COX-2 with a low micromolar inhibitor (compound **3e**) reasserted its dynamic stability throughout the simulation run. It also substantiated that the binding interactions predicted by docking studies were stable. This exercise reaffirmed the selective COX-2 inhibition of the compound **3e** and its anti-inflammatory activity.

2.3.3. *In Silico estimation of “drug-like” properties & Partition co-efficient*

Prediction of “drug-likeness” for the most active compounds was carried out using QikProp module of Schrödinger Maestro 10.5.014. The predicted outcome of some important parameters including Log P is reported in **Table 9**. The experimental Log P values (**Table 1**) were found in the range of 3.44-4.58 with the mean Log P value of 4.10 and vary with those predicted *in silico*. However, no strong correlation could be drawn between lipophilicity and COX-2 inhibitory activity. Nevertheless, the experimental Log P values conform to ≤ 5 which is in compliance with Lipinski's rule of five [52] to ascertain whether a chemical compound with certain pharmacological activity is endowed with properties that would make it a likely orally active drug in humans. Amongst the calculated parameters, the number of rotatable bonds (#rotor) provides a prediction for the conformational flexibility of the molecule, which in turn, decides the binding to its target protein. Polar surface area (PSA) is another important parameter used in estimating the drug transporter properties. PSA is the sum of surfaces of polar atoms such as oxygen, nitrogen, and attached hydrogen. Along with Lipinski's rule of five, these two parameters are vital in achieving a good oral bioavailability [53].

Of the other predicted parameter, QPPCaco predicts for the non-active transport for the gut-blood barrier using Caco-2 cells as a model. It reflects the compound's ability to get efficiently distributed inside the body. Except for compounds **3e** (83.31) and **4e** (109.31), which exhibited moderate permeability, remaining compounds displayed an excellent Caco-2 permeability. The amount of protein binding of drugs is an important pharmacokinetic consideration. The predicted QPlogKhsa values affirm their strong binding with plasma protein. All the compounds under study displayed a good human (72%-100%) oral absorption. The outcome of Lipinski's rule of five (mol_MW<500, QPlog Po/w < 5, donorHB 0-6.0, accptHB 2.0-20), along with the other predicted parameters indicated that the compounds under consideration (**3c-3e** and **4c-4e**) did elicit “drug-like” characteristics.

Table 9 Predicted drug likeliness properties for the most active compounds

Compound	Mol_MW (130-725)	#rotor (0-15)	PSA (7-200)	donor HB (0-6)	accept HB (2-20)	QPlog Po/w (-2-6.5)	QPP Caco (<25 poor, >500 great)	QPlog Khsa (-1.5- 1.5)	% Human oral absorption >80% high, <25% poor)	Rule of five (Max 4)
3c	452.47	8	19.37	1	6.75	4.84	696.47	0.669	100.00	0
3d	456.89	7	101.11	1	6.00	5.28	725.87	0.789	96.10	1
3e	467.44	8	146.00	1	7.00	4.05	83.31	0.611	72.08	1
4c	468.53	8	97.61	1	6.25	5.54	953.73	0.875	100.00	1
4d	472.95	7	89.28	1	5.50	5.94	914.51	0.994	100.00	1
4e	483.50	8	134.22	1	6.50	4.73	109.31	0.816	91.13	0

Mol_MW: molecular weight

#rotor: No. of rotatable bonds

donorHB: No. of hydrogen bonds that would be donated by the solute to water molecules in an aqueous solution

acceptHB: No. of hydrogen bonds that would be accepted by the solute from water molecules in an aqueous solution

QPlogPo/w: Predicted octanol/water partition coefficient

QPPCaco: Caco-2 cell permeability in nm sec⁻¹

QPlogKhsa: binding to human serum albumin

Percent Human-Oral Absorption: human oral absorption on 0 to 100% scale

PSA: polar surface area

Rule of five: No. of violations of Lipinski's rule of five

3. Conclusion

A series of fifteen novel compounds were designed and synthesised by hybridising the 5,6-diphenyl-1,2,4-triazine moiety with a 1,3,4-oxadiazole/thiadiazole and 1,2,4-triazole scaffold. Derivatives **3c-3e** and **4c-4e** exhibited *in vivo* anti-inflammatory activity by inhibiting the exudative and transudative stages of inflammation with commendable gastric, hepatic and renal safety profiles. *In vitro* mechanistic studies revealed the competitive nature of the selective COX-2 inhibition by the potential compounds. Hybrids comprising of 5,6-diaryl 1,2,4-triazine ring bearing a 1,3,4-oxadiazole nucleus (**3c-3e**) were marginally more effective selective COX-2 inhibitors as compared to their 1,3,4-thiadiazole (**4c-4e**) counterpart. Based on the outcome of *in vitro* COX assay compounds **3e** and **4c** were evaluated and found devoid of cardiotoxicity on myocardial infarcted rats. The *in silico* studies displayed their consensual binding within the COX-2 active site. It also helped to explain the geometric requisites of the "hybrid-pharmacophore" conducive for COX-2 inhibition which was absent in compounds **5a-5e**. In conclusion, compounds **3c-3e** consisting of a 1,3,4-oxadiazole ring and **4c-4e** comprising of its bioisosteric 1,3,4-thiadiazole counterpart bearing an electron withdrawing methoxy, chloro and nitro group on its para position

and tethered to a 5,6-diphenyl-1,2,4-triazin-3(2*H*)-one moiety can serve as a propitious scaffold for the development of newer and safer selective COX-2 inhibitory agents.

4. Experimental

4.1. Chemistry

Chemicals and solvents used were of analytical grade. The progress of the reactions was monitored by thin layer chromatography (TLC) on pre-coated Merck silica gel 60 F254 aluminium sheets (Merck, Germany). Melting points were determined using open capillary tubes on a Stuart melting point apparatus (SMP10) and were uncorrected. FT-IR spectra were recorded on a Shimadzu 8400S FT-IR spectrophotometer. ¹H NMR (300 MHz and 500 MHz) and ¹³C NMR (75 MHz and 125 MHz) were recorded on a JEOL AL300 FT-NMR and JEOL AL500 FT-NMR in DMSO-*d*₆ using TMS as an internal standard. C, H, N analyses were performed on an Exeter CE-440 elemental analyser.

4.1.1 General procedure for the synthesis of 2-(3-Oxo-5,6-diphenyl-1,2,4-triazin-2(3*H*)-yl)acetohydrazide (**1**).

Intermediate (**1**) was synthesized from Ethyl 2-(3-oxo-5,6-diphenyl-1,2,4-triazin-2(3*H*)-yl)acetate with slight modifications to the reported procedure [54]. Ethyl 2-(3-oxo-5,6-diphenyl-1,2,4-triazin-2(3*H*)-yl)acetate (0.6 g, 1.789 mmol) (1 Mol. Eq.) was dissolved in 10 ml methanol by heating at around 60 °C. To this solution, hydrazine hydrate (4 Mol. Eq.) was added drop wise. The reaction mixture was refluxed for 2 h instead of reported 1 h with the progress being monitored by TLC using DCM/Methanol (2:8) as the mobile phase. After completion, the reaction mixture was poured over crushed ice. The solid that separated was filtered dried and recrystallised from ethanol to yield the title compound **1**.

Yield: 0.468 g, 78%; mp 171-173 °C (from EtOH); R_f 0.39. FT-IR (KBr, cm⁻¹): 3408, 3294 and 3209 (NH); 3057, 2925 (CH); 1678 (CO); 1541 (CN). ¹H NMR (300 MHz, DMSO-*d*₆, ppm): δ 8.03 (s, 1H, NH); δ 7.26–7.72 (m, 10H, Ar-H); δ 4.47 (bs, 2H, NH₂); δ 3.34 (s, 2H, CH₂CO). ¹³C NMR (75 MHz, DMSO-*d*₆, ppm): 165.43, 160.82, 155.68, 151.45, 142.55, 136.24, 135.20, 130.53, 129.32, 128.62, 127.01, 125.72, 55.05. Anal. calc. for C₁₇H₁₅N₅O₂: C, 63.54; H, 4.71; N, 21.79%; Found: C, 63.74; H, 4.69; N, 21.85.

4.1.2. General procedure for the synthesis of compounds (**2a-2e**).

2-(3-Oxo-5,6-diphenyl-1,2,4-triazin-2(3*H*)-yl)acetohydrazide (0.5 g, 1.55 mmol) (1 Mol. Eq.) (**1**) was dissolved in aq. ethanol (75% v/v) with gentle heating at around 70°C. Various

phenyl/substituted phenyl isothiocyanate derivatives (1.5 Mol. Eq.) were added to the above mixture in small portions with stirring. The reaction was allowed to proceed at room temperature with stirring (12-15 h). The progress of the reaction was monitored by TLC with DCM/Methanol (9.0:1.0) as the mobile phase. After completion, the reaction mixture was filtered, and the precipitate was washed with a small amount (3x5 ml) of ethyl acetate (EtOAc) to remove away any unreacted isothiocyanate. The residual EtOAc layer was evaporated in a rotary vacuum evaporator to yield the title compounds (**2a-2e**).

4.1.2.1. *1-(2-(3-Oxo-5,6-diphenyl-1,2,4-triazin-2(3H)-yl)acetyl)-4-phenylthiosemicarbazide (2a)*

Yield: 0.380 g, 76%; mp 202-204 °C; R_f 0.44. FT-IR (KBr, cm^{-1}): 3211 and 3113 (NH); 3005 and 2941 (CH); 1699 (CO); 1546 (CN); 1192 (CS). ^1H NMR (300 MHz, DMSO- d_6 , ppm): δ 3.86 (s, 2H, methylene); δ 7.13–7.53 (m, 15H, Ar-H); δ 8.53 (s, 1H, NH exchangeable with D_2O); δ 9.86 (s, 1H, CSNH exchangeable with D_2O); δ 10.51 (s, 1H, CONH exchangeable with D_2O). ^{13}C NMR (75 MHz, DMSO- d_6 , ppm): 54.77, 124.85, 125.23, 128.17, 128.30, 128.96, 129.16, 129.43, 131.20, 133.84, 135.12, 138.78, 138.91, 139.00, 139.11, 142.66, 152.81, 165.90, 167.04, 172.02, 180.63. Anal. calc. for $\text{C}_{24}\text{H}_{20}\text{N}_6\text{O}_2\text{S}$ C, 63.14; H, 4.42; N, 18.41%; Found: C, 63.37; H, 4.44; N, 18.48.

4.1.2.2. *1-(2-(3-Oxo-5,6-diphenyl-1,2,4-triazin-2(3H)-yl)acetyl)-4-p-tolylthiosemicarbazide (2b)*

Yield: 0.365 g, 73%; mp 211-213 °C; R_f 0.47. FT-IR (KBr, cm^{-1}): 3109 and 3201 (NH); 3026 and 2941 (CH); 1664 (CO); 1545 (CN); 1193 (CS). ^1H NMR (300 MHz, DMSO- d_6 , ppm): δ 2.24 (s, 3H, methyl); δ 3.82 (s, 2H, methylene); δ 7.17–7.51 (m, 14H, Ar-H); δ 8.52 (s, 1H, NH exchangeable with D_2O); δ 9.71 (s, 1H, CSNH exchangeable with D_2O); δ 10.52 (s, 1H, CONH exchangeable with D_2O). ^{13}C NMR (75 MHz, DMSO- d_6 , ppm): 25.14, 54.72, 126.36, 127.64, 127.92, 128.24, 129.11, 130.01, 130.36, 130.48, 133.54, 134.03, 137.42, 139.20, 142.52, 154.09, 165.33, 167.71, 172.12, 182.21. Anal. calc. for $\text{C}_{25}\text{H}_{22}\text{N}_6\text{O}_2\text{S}$ C, 63.81; H, 4.71; N, 17.86%; Found: C, 64.05; H, 4.76; N, 17.92.

4.1.2.3. *4-(4-Methoxyphenyl)-1-(2-(3-oxo-5,6-diphenyl-1,2,4-triazin-2(3H)-yl)acetyl)thiosemicarbazide (2c)*

Yield: 0.385 g, 77%; mp 218-220 °C; R_f 0.45. FT-IR (KBr, cm^{-1}): 3213 and 3120 (NH); 3003, 2949 and 2837 (CH); 1664 (CO); 1545 (CN); 1209 (CS). ^1H NMR (300 MHz, DMSO- d_6 , ppm): δ 3.73 (s, 3H, methoxy); δ 3.78 (s, 2H, methylene); δ 7.08–7.39 (m, 14H, Ar-H); δ 8.46 (s, 1H, NH exchangeable with D_2O); δ 9.86 (s, 1H, CSNH exchangeable with D_2O); δ 10.51 (s, 1H, CONH exchangeable with D_2O). ^{13}C NMR (75 MHz, DMSO- d_6 , ppm): 55.06, 55.13, 116.68, 128.15,

128.27, 128.95, 129.16, 129.41, 131.19, 133.83, 135.11, 140.04, 140.18, 142.66, 152.81, 159.08, 165.86, 167.05, 172.95, 180.77. Anal. calc. for C₂₅H₂₂N₆O₃S: C, 61.71; H, 4.56; N, 17.27%; Found: C, 61.94; H, 4.57; N, 17.32.

4.1.2.4. *4-(4-Chlorophenyl)-1-(2-(3-oxo-5,6-diphenyl-1,2,4-triazin-2(3H)-yl)acetyl)thiosemicarbazide (2d)*

Yield: 0.415 g, 83%; mp 215-216 °C; R_f 0.46. FT-IR (KBr, cm⁻¹): 3238 and 3109 (NH); 3057 and 2989 (CH); 1608 (CO); 1546 (CN); 1203 (CS). ¹H NMR (300 MHz, DMSO-*d*₆, ppm): δ 3.83 (s, 2H, methylene); δ 7.29–7.58 (m, 14H, Ar–H); δ 8.56 (s, 1H, NH exchangeable with D₂O); δ 9.96 (s, 1H, CSNH exchangeable with D₂O); δ 10.51 (s, 1H, CONH exchangeable with D₂O). ¹³C NMR (75 MHz, DMSO-*d*₆, ppm): 54.70, 126.80, 127.95, 128.04, 128.13, 128.27, 128.93, 129.13, 129.41, 131.17, 133.81, 135.09, 137.87, 138.15, 142.61, 152.75, 165.87, 167.00, 172.60, 181.51. Anal. calc. for C₂₄H₁₉ClN₆O₂S: C, 58.71; H, 3.90; N, 17.12%; Found: C, 58.69; H, 3.91; N, 17.16.

4.1.2.5. *4-(4-Nitrophenyl)-1-(2-(3-oxo-5,6-diphenyl-1,2,4-triazin-2(3H)-yl)acetyl)thiosemicarbazide (2e)*

Yield: 0.400 g, 80%; mp 225-226 °C; R_f 0.42. FT-IR (KBr, cm⁻¹): 3288 (NH); 3078 and 2991 (CH); 1670 (CO); 1562 (CN); 1332 (NO); 1205 (CS). ¹H NMR (300 MHz, DMSO-*d*₆, ppm): δ 3.85 (s, 2H, methylene); δ 7.30–7.39 (m, 10H, Ar–H); δ 7.97 (s, 2H, Ar–H); δ 8.20–8.23 (d, 2H, Ar–H); δ 8.56 (s, 1H, NH exchangeable with D₂O); δ 9.95 (s, 1H, CSNH exchangeable with D₂O); δ 10.63 (s, 1H, CONH exchangeable with D₂O). ¹³C NMR (75 MHz, DMSO-*d*₆, ppm): 54.81, 125.46, 128.13, 128.27, 128.93, 129.15, 129.41, 131.19, 133.80, 135.07, 142.66, 143.39, 145.35, 152.80, 155.96, 165.93, 167.05, 173.02, 180.32. Anal. calc. for C₂₄H₁₉N₇O₄S: C, 57.48; H, 3.82; N, 19.55%; Found: C, 57.70; H, 3.84; N, 19.62.

4.1.3. *General procedure for the synthesis of compounds (3a-3e).*

A suspension of intermediate (**2a-2e**) (0.4g, 1 Mol. Eq.) in 25 ml of ethanol was dissolved in 1 ml of 5N aq. NaOH with cooling at around 30°C and stirring resulting in a clear solution. To this, iodine in potassium iodide solution (5%) was added gradually with stirring till the colour of the iodine persisted at room temperature. The reaction mixture was then refluxed for 1 h. The progress of the reaction was monitored by TLC with DCM/Methanol (9.5:0.5) as the mobile phase. After completion, the contents of the beaker were poured over crushed ice. The solid that separated was filtered dried and recrystallised from ethanol to yield the title compounds (**3a-3e**).

4.1.3.1. *5,6-Diphenyl-2-((5-(phenylamino)-1,3,4-oxadiazol-2-yl)methyl)-1,2,4-triazin-3(2H)-one (3a)*

Yield: 0.276 g, 69%. FT-IR (KBr, cm^{-1}): 3363 (NH); 2926 (CH); 1599 (CO); 1548 (CN); 1016 (COC). ^1H NMR (300 MHz, DMSO- d_6 , ppm): δ 4.21 (s, 2H, methylene); δ 6.88–6.93 (t, 1H, Ar-H); δ 7.20–7.31 (m, 2H, Ar-H); δ 7.39–7.41 (m, 8H, Ar-H); δ 7.43–7.57 (m, 4H, Ar-H); δ 8.33 (s, 1H, NH exchangeable with D_2O). ^{13}C NMR (75 MHz, DMSO- d_6 , ppm): 53.32, 117.68, 122.10, 124.84, 126.61, 128.22, 129.12, 129.44, 131.12, 133.85, 135.16, 139.15, 140.41, 141.54, 142.85, 152.85, 165.77, 167.19. Anal. calc. for $\text{C}_{24}\text{H}_{18}\text{N}_6\text{O}_2$: C, 68.24; H, 4.29; N, 19.89%; Found: C, 68.50; H, 4.31; N, 19.97.

4.1.3.2. *2-((5-(p-Tolylamino)-1,3,4-oxadiazol-2-yl)methyl)-5,6-diphenyl-1,2,4-triazin-3(2H)-one (3b)*

Yield: 0.284 g, 71%. FT-IR (KBr, cm^{-1}): 3367 (NH); 2924 (CH); 1618 (CO); 1114 (COC). ^1H NMR (300 MHz, DMSO- d_6 , ppm): δ 2.25 (s, 2H, methyl); δ 4.23 (s, 2H, methylene); δ 6.98–7.45 (m, 15H, Ar-H); δ 8.36 (s, 1H, NH exchangeable with D_2O). ^{13}C NMR (75 MHz, DMSO- d_6 , ppm): 25.65, 54.03, 120.27, 121.04, 123.20, 123.97, 125.76, 126.46, 128.25, 128.82, 130.05, 130.55, 130.66, 135.02, 137.87, 139.15, 145.26, 146.42, 152.16, 157.87, 165.86, 167.38. Anal. calc. for $\text{C}_{25}\text{H}_{20}\text{N}_6\text{O}_2$: C, 68.80; H, 4.62; N, 19.25%; Found: C, 68.52; H, 4.60; N, 19.18.

4.1.3.3. *2-((5-(4-Methoxyphenylamino)-1,3,4-oxadiazol-2-yl)methyl)-5,6-diphenyl-1,2,4-triazin-3(2H)-one (3c)*

Yield: 0.304 g, 76%. FT-IR (KBr, cm^{-1}): 3372 (NH); 2933, 2835 (CH); 1606 (CO); 1558 (CN); 1030 (COC). ^1H NMR (300 MHz, DMSO- d_6 , ppm): δ 3.69 (s, 3H, methoxy); δ 4.33 (s, 2H, methylene); δ 7.06–7.63 (m, 14H, Ar-H); δ 8.36 (s, 1H, NH exchangeable with D_2O). ^{13}C NMR (75 MHz, DMSO- d_6 , ppm): 54.29, 55.32, 119.58, 122.88, 125.96, 126.29, 127.90, 128.06, 121.19, 129.51, 129.83, 130.16, 130.25, 130.52, 130.66, 131.04, 133.65, 136.02, 142.32, 147.90, 156.22, 165.00, 167.83. Anal. calc. for $\text{C}_{25}\text{H}_{20}\text{N}_6\text{O}_3$: C, 66.36; H, 4.46; N, 18.57%; Found: C, 66.60; H, 4.48; N, 18.64.

4.1.3.4. *2-((5-(4-Chlorophenylamino)-1,3,4-oxadiazol-2-yl)methyl)-5,6-diphenyl-1,2,4-triazin-3(2H)-one (3d)*

Yield: 0.320 g, 80%. FT-IR (KBr, cm^{-1}): 3403 (NH); 2928 (CH); 1614 (CO); 1554 (CN); 1091 (COC). ^1H NMR (300 MHz, DMSO- d_6 , ppm): δ 4.25 (s, 2H, methylene); δ 6.98–7.70 (m, 14H, Ar-H); δ 8.43 (s, 1H, NH exchangeable with D_2O). ^{13}C NMR (75 MHz, DMSO- d_6 , ppm): 54.16, 118.97, 124.62, 125.43, 128.08, 128.24, 128.79, 128.90, 128.97, 129.18, 129.46, 131.13, 133.85,

135.16, 138.63, 139.29, 139.83, 142.90, 152.15, 165.63, 167.22. Anal. calc. for $C_{24}H_{17}ClN_6O_2$: C, 63.09; H, 3.75; N, 18.39%; Found: C, 63.33; H, 3.76; N, 18.46.

4.1.3.5. *2-((5-(4-Nitrophenylamino)-1,3,4-oxadiazol-2-yl)methyl)-5,6-diphenyl-1,2,4-triazin-3(2H)-one (3e)*

Yield: 0.316 g, 79%. FT-IR (KBr, cm^{-1}): 3365 (NH); 3086 and 2926 (CH); 1627 (CO); 1593 (CN), 1332 (NO); 1111 (COC). 1H NMR (300 MHz, DMSO- d_6 , ppm): δ 4.29 (s, 2H, methylene); δ 7.26–7.38 (m, 9H, Ar–H); δ 7.78–7.81 (d, 2H, Ar–H); δ 8.19 (s, 1H, Ar–H); δ 8.41 (s, 2H, Ar–H); δ 8.42 (s, 1H, NH exchangeable with D_2O). ^{13}C NMR (75 MHz, DMSO- d_6 , ppm): 53.37, 117.02, 125.46, 127.90, 128.10, 128.27, 128.99, 129.22, 129.48, 131.18, 133.85, 135.16, 140.92, 142.97, 146.12, 152.19, 154.80, 164.97, 167.27. Anal. calc. for $C_{24}H_{17}N_7O_4$: C, 61.67; H, 3.67; N, 20.98%; Found: C, 61.90; H, 3.66; N, 20.91.

4.1.4. *General procedure for the synthesis of compounds (4a-4e).*

Intermediates (**2a-2e**) (0.4g, 1 Mol. Eq.) were added gradually with stirring to a cold solution of concentrated sulphuric acid (10 ml). The reaction mixture was stirred for 4-6 h in an ice bath. The progress of the reaction was monitored by TLC with DCM/Methanol (9.5:0.5) as the mobile phase. After completion, the contents of the beaker were poured over crushed ice and the solid thus separated was filtered, washed with water, and recrystallised from ethanol to yield the title compounds (**4a-4e**).

4.1.4.1. *5,6-Diphenyl-2-((5-(phenylamino)-1,3,4-thiadiazol-2-yl)methyl)-1,2,4-triazin-3(2H)-one (4a)*

Yield: 0.280 g, 70%. FT-IR (KBr, cm^{-1}): 3205 (NH); 2939 (CH); 1658 (CO); 1599 (CN). 1H NMR (300 MHz, DMSO- d_6 , ppm): δ 4.28 (s, 2H, methylene); δ 6.95–7.52 (m, 15H, Ar–H); δ 8.37 (s, 1H, NH exchangeable with D_2O). ^{13}C NMR (75 MHz, DMSO- d_6 , ppm): 54.02, 117.68, 122.10, 124.83, 126.60, 128.21, 129.11, 129.30, 131.11, 133.83, 135.12, 139.13, 140.30, 141.44, 142.72, 153.75, 165.97, 167.29. Anal. calc. for $C_{24}H_{18}N_6OS$: C, 65.74; H, 4.14; N, 19.17%; Found: C, 65.98; H, 4.15; N, 19.24.

4.1.4.2. *2-((5-(p-Tolylamino)-1,3,4-thiadiazol-2-yl)methyl)-5,6-diphenyl-1,2,4-triazin-3(2H)-one (4b)*

Yield: 0.296 g, 74%. FT-IR (KBr, cm^{-1}): 3309 (NH); 2928 (CH); 1558 (CO); 1527 (CN). 1H NMR (300 MHz, DMSO- d_6 , ppm): δ 2.25 (s, 3H, methyl); δ 4.32 (s, 2H, methylene); δ 6.94–7.02 (m, 2H, Ar–H); δ 7.15–7.26 (m, 10H, Ar–H); δ 7.63–7.65 (d, 1H, Ar–H); δ 7.80–7.83 (d, 1H, Ar–H); δ

8.41 (s, 1H, NH exchangeable with D₂O). ¹³C NMR (75 MHz, DMSO-*d*₆, ppm): 54.03, 120.27, 121.07, 123.20, 123.97, 125.77, 126.47, 128.27, 128.85, 130.07, 130.57, 130.67, 135.02, 137.87, 139.15, 145.26, 146.44, 152.17, 157.88, 166.55, 168.28 Anal. calc. for C₂₅H₂₀N₆OS: C, 66.35; H, 4.45; N, 18.57%; Found: C, 66.08; H, 4.43; N, 18.51.

4.1.4.3. 2-((5-(4-Methoxyphenylamino)-1,3,4-thiadiazol-2-yl)methyl)-5,6-diphenyl-1,2,4-triazin-3(2H)-one (**4c**)

Yield: 0.296 g, 74%. FT-IR (KBr, cm⁻¹): 3381 (NH); 2902 (CH); 1664 (CO); 1585 (CN). ¹H NMR (300 MHz, DMSO-*d*₆, ppm): δ 3.72 (s, 3H, methoxy); δ 4.29 (s, 2H, methylene); δ 7.26–7.69 (m, 14H, Ar-H); δ 8.36 (s, 1H, NH exchangeable with D₂O). ¹³C NMR (75 MHz, DMSO-*d*₆, ppm): 54.50, 55.26, 119.80, 123.05, 126.11, 126.50, 128.13, 128.39, 129.50, 129.80, 130.00, 130.46, 130.56, 130.86, 130.96, 131.40, 133.91, 136.44, 142.60, 148.22, 156.92, 165.60, 168.62. Anal. calc. for C₂₅H₂₀N₆O₂S: C, 64.09; H, 4.30; N, 17.94%; Found: C, 64.33; H, 4.28; N, 17.99.

4.1.4.4. 2-((5-(4-Chlorophenylamino)-1,3,4-thiadiazol-2-yl)methyl)-5,6-diphenyl-1,2,4-triazin-3(2H)-one (**4d**)

Yield: 0.308 g, 77%. FT-IR (KBr, cm⁻¹): 3257 (NH); 3055 (CH); 1658 (CO); 1599 (CN). ¹H NMR (300 MHz, DMSO-*d*₆, ppm): δ 4.27 (s, 2H, methylene); δ 7.28–8.21 (m, 14H, Ar-H); δ 8.40 (s, 1H, NH exchangeable with D₂O). ¹³C NMR (75 MHz, DMSO-*d*₆, ppm): 54.36, 118.98, 124.62, 125.43, 128.07, 128.24, 128.78, 128.90, 128.98, 129.18, 129.47, 131.13, 133.85, 135.17, 138.63, 139.29, 139.83, 142.89, 152.15, 165.68, 167.23. Anal. calc. for C₂₄H₁₇ClN₆OS: C, 60.95; H, 3.62; N, 17.77%; Found: C, 61.18; H, 3.63; N, 17.70.

4.1.4.5. 2-((5-(4-Nitrophenylamino)-1,3,4-thiadiazol-2-yl)methyl)-5,6-diphenyl-1,2,4-triazin-3(2H)-one (**4e**)

Yield: 0.320 g, 80%. FT-IR (KBr, cm⁻¹): 3259 (NH); 3059 (CH); 1651 (CO); 1597 (CN); 1330 (NO). ¹H NMR (300 MHz, DMSO-*d*₆, ppm): δ 4.26 (s, 2H, methylene); δ 7.36–7.81 (m, 9H, Ar-H); δ 7.82–7.95 (m, 3H, Ar-H); δ 8.05–8.40 (m, 2H, Ar-H); δ 8.42 (s, 1H, NH exchangeable with D₂O). ¹³C NMR (75 MHz, DMSO-*d*₆, ppm): 54.05, 116.92, 125.42, 127.86, 128.06, 128.22, 128.92, 129.19, 129.44, 131.12, 133.81, 135.11, 140.89, 142.92, 146.10, 152.10, 154.79, 165.37, 168.07. Anal. calc. for C₂₄H₁₇N₇O₃S: C, 59.62; H, 3.54; N, 20.28%; Found: C, 59.84; H, 3.55; N, 20.36.

4.1.5. General procedure for the synthesis of compounds (**5a-5e**).

A suspension of intermediates (**2a-2e**) (0.4g, 1 Mol. Eq.) in 25 ml of absolute ethanol was dissolved in aq. NaOH (4N, 2 ml) and gently refluxed for 2 h. The progress of the reaction was monitored by TLC with DCM/Methanol (9.5:0.5) as the mobile phase. After completion, the resulting solution was cooled, concentrated and filtered. The pH of the filtrate was adjusted between 5-6 with dilute acetic acid (40% v/v) and kept aside for 1 h to afford the compounds (**5a-5e**). The crude product was filtered, washed with water, dried and recrystallised from ethanol.

4.1.5.1. *2-((5-Mercapto-4-phenyl-4H-1,2,4-triazol-3-yl)methyl)-5,6-diphenyl-1,2,4-triazin-3(2H)-one (5a)*

Yield: 0.288 g, 72%. FT-IR (KBr, cm^{-1}): 2928 (CH); 1597 (CO); 1543 (CN). ^1H NMR (500 MHz, DMSO- d_6 , ppm): δ 4.25 (s, 2H, methylene); δ 7.17–7.53 (m, 15H, Ar-H); δ 11.27 (s, 1H, SH exchangeable with D_2O). ^{13}C NMR (125 MHz, DMSO- d_6 , ppm): 54.23, 118.31, 121.91, 125.84, 128.72, 129.03, 129.17, 129.47, 129.84, 129.94, 130.17, 130.37, 130.72, 130.81, 131.12, 133.21, 134.17, 141.39, 142.47, 148.68, 159.18, 165.27, 167.27. Anal. calc. for $\text{C}_{24}\text{H}_{18}\text{N}_6\text{OS}$: C, 65.74; H, 4.14; N, 19.17%; Found: C, 65.89; H, 4.15; N, 19.20.

4.1.5.2. *2-((5-Mercapto-4-p-tolyl-4H-1,2,4-triazol-3-yl)methyl)-5,6-diphenyl-1,2,4-triazin-3(2H)-one (5b)*

Yield: 0.288 g, 72%. FT-IR (KBr, cm^{-1}): 2926 (CH); 1618 (CO); 1593 (CN). ^1H NMR (300 MHz, DMSO- d_6 , ppm): δ 2.24 (s, 3H, methyl); δ 4.26 (s, 2H, methylene); δ 6.98–7.47 (m, 14H, Ar-H); δ 11.27 (s, 1H, SH exchangeable with D_2O). ^{13}C NMR (75 MHz, DMSO- d_6 , ppm): 25.24, 53.68, 119.63, 122.45, 123.16, 124.30, 126.24, 126.41, 127.07, 127.43, 129.43, 129.92, 130.36, 130.42, 130.95, 131.03, 131.63, 136.79, 137.73, 149.57, 159.67, 165.03, 168.62. Anal. calc. for $\text{C}_{25}\text{H}_{20}\text{N}_6\text{OS}$: C, 66.35; H, 4.45; N, 18.57%; Found: C, 66.48; H, 4.46; N, 18.61.

4.1.5.3. *2-((5-Mercapto-4-(4-methoxyphenyl)-4H-1,2,4-triazol-3-yl)methyl)-5,6-diphenyl-1,2,4-triazin-3(2H)-one (5c)*

Yield: 0.312 g, 78%. FT-IR (KBr, cm^{-1}): 2935 (CH); 1606 (CO); 1552 (CN). ^1H NMR (300 MHz, DMSO- d_6 , ppm): δ 3.73 (s, 3H, methoxy); δ 4.25 (s, 2H, methylene); δ 6.46–7.46 (m, 14H, Ar-H); δ 11.26 (s, 1H, SH exchangeable with D_2O). ^{13}C NMR (75 MHz, DMSO- d_6 , ppm): 54.92, 55.39, 116.91, 121.18, 122.30, 125.11, 128.50, 128.68, 129.21, 129.35, 130.16, 133.55, 136.04, 137.86, 141.23, 148.03, 159.61, 162.61, 165.21, 168.55. Anal. calc. for $\text{C}_{25}\text{H}_{20}\text{N}_6\text{O}_2\text{S}$: C, 64.09; H, 4.30; N, 17.94%; Found: C, 63.92; H, 4.29; N, 17.89.

4.1.5.4. 2-((4-(4-Chlorophenyl)-5-mercapto-4H-1,2,4-triazol-3-yl)methyl)-5,6-diphenyl-1,2,4-triazin-3(2H)-one (**5d**)

Yield: 0.320 g, 80%. FT-IR (KBr, cm^{-1}): 2928 (CH); 1703 (CO); 1546 (CN). ^1H NMR (500 MHz, DMSO- d_6 , ppm): δ 4.28 (s, 2H, methylene); δ 7.22–7.91 (m, 14H, Ar-H); δ 11.26 (s, 1H, SH exchangeable with D_2O). ^{13}C NMR (125 MHz, DMSO- d_6 , ppm): 54.27, 119.89, 125.54, 127.69, 128.17, 129.08, 129.61, 130.34, 130.68, 131.33, 131.63, 131.99, 133.37, 134.84, 139.42, 141.75, 148.40, 159.26, 165.73, 168.93. Anal. calc. for $\text{C}_{24}\text{H}_{17}\text{ClN}_6\text{OS}$: C, 60.95; H, 3.62; N, 17.77%; Found: C, 60.83; H, 3.61; N, 17.73.

4.1.5.5. 2-((5-Mercapto-4-(4-nitrophenyl)-4H-1,2,4-triazol-3-yl)methyl)-5,6-diphenyl-1,2,4-triazin-3(2H)-one (**5e**)

Yield: 0.316 g, 79%. FT-IR (KBr, cm^{-1}): 3099 (CH); 1593 (CO); 1506 (CN); 1330 (NO). ^1H NMR (500 MHz, DMSO- d_6 , ppm): δ 4.28 (s, 2H, methylene); δ 7.13–7.54 (m, 10H, Ar-H); δ 7.46–7.76 (d, 2H, Ar-H); δ 8.14–8.20 (d, 2H, Ar-H); δ 11.31 (s, 1H, SH exchangeable with D_2O). ^{13}C NMR (125 MHz, DMSO- d_6 , ppm): 54.57, 119.46, 125.24, 127.59, 127.95, 128.14, 128.32, 128.66, 128.96, 129.11, 129.39, 129.87, 130.25, 130.93, 131.13, 131.47, 133.03, 134.07, 139.70, 141.21, 148.57, 159.45, 166.13, 169.09. Anal. calc. for $\text{C}_{24}\text{H}_{17}\text{N}_7\text{O}_3\text{S}$: C, 59.62; H, 3.54; N, 20.28%; Found: C, 59.73; H, 3.55; N, 20.31.

4.2. Determination of partition coefficient

The lipophilic constant of all of the compounds (**2a-2e**, **3a-3e**, **4a-4e** and **5a-5e**) was determined in *n*-octanol and buffer (pH 7.4) by the shake flask method [55]. The log P was calculated by correlating the absorbance with the concentration using a standard plot.

4.3. Pharmacology

4.3.1. Animals

Healthy Swiss albino rats (180-200 g) and mice (20-30 g) of either sex were procured from the Central Animal House, Institute of Medical Sciences, Banaras Hindu University. Animals were housed in polypropylene cages maintained at a room temperature of 22 ± 3 °C and 45% relative humidity under 12 h light/dark ambience. Animals had free access to commercial pellet diet and water *ad libitum*. The synthesised derivatives (0.0279 mmol kg^{-1}) and standard drugs (indomethacin/ celecoxib) (0.0279 mmol kg^{-1}) were administered as suspensions consisting of 0.3% sodium carboxymethylcellulose (CMC) in distilled water. The *in vivo* experimental protocol was duly approved by the Central Animal Ethical Committee of BHU, Varanasi, India (Protocol No.

Dean/13–14/CAEC/320). Experiments involving animals have been reported according to ARRIVE guidelines [56].

4.3.2. *In vitro* anti-inflammatory screening (Albumin denaturation assay) [57]

Indomethacin, celecoxib, and hybrids (**2a-2e**, **3a-3e**, **4a-4e** and **5a-5e**) were dissolved in a minimum amount of dimethyl formamide (DMF) and diluted with phosphate-buffered saline (pH 7.4) maintaining the concentration of DMF in all solutions less than 2.5%. Test solutions (1 ml, 100 mg ml⁻¹) were mixed with 1 ml of 1% w/v albumin in phosphate-buffered saline and incubated at 27 ± 1 °C for 15 min. Denaturation was induced by heating the mixture at 60 ± 1 °C for 10 min. After cooling, the turbidity was measured at 660 nm. The percent inhibition of denaturation was calculated from the control, where no drug was added. Each experiment was performed in triplicate, and an average was taken.

The percent inhibition was calculated using the formula

$$\% \text{ Inhibition of denaturation} = [(V_t/V_c) - 1] \times 100$$

Where V_t = means absorption of test compound and

V_c = means absorption of control

4.3.3. *Acute oral toxicity studies*

Based on the outcome of preliminary *in vitro* assessment, acute oral toxicity studies of selected compounds (**3c-3e**, **4c-4e**, **5d** and **5e**) were performed on nulliparous, non-pregnant, healthy female albino rats as per OECD-425, 2001 guidelines [58]. Compounds were administered in graded doses ranging from 100-500 mg kg⁻¹, *p.o.* The animals were monitored continuously for 24 h for any changes in their autonomic or behavioural responses and also for tremors, convulsion, salivation, diarrhoea, lethargy, sleep and coma and then monitored for mortality, if any, for the following 14 days.

4.3.4. *Carrageenan-induced rat paw oedema* [59]

Acute inflammation was produced by the sub-plantar administration of 0.1 ml of a 1% w/v solution of lambda carrageenan in normal saline on the left hind paw of the rats. Different groups were pre-treated orally with standard drugs (indomethacin/celecoxib) or selected compounds (**3c-3e**, **4c-4e**, **5d** and **5e**) 1 h before the administration of carrageenan. The total increase in the paw volume was measured at 1 h intervals till 6 h post carrageenan injection using a digital Vernier calliper (*Mitutoyo*).

4.3.5. *Cotton pellet induced granuloma in rats* [60]

After shaving, rats were anaesthetized and autoclaved cotton pellets each weighing 35 ± 1 mg were implanted subcutaneously through a small incision made in the axilla. Different groups of the animals received standard drugs (indomethacin/ celecoxib) and selected hybrids (**3c-3e** and **4c-4e**) once daily for seven consecutive days from the day of pellet implantation. On the eighth day, the cotton pellets covered by the granulomatous tissue were excised and dried at $60\text{ }^{\circ}\text{C}$ to a constant weight. Increments in the dry weight of the pellets were considered as a measure of granuloma formation.

4.3.6. Freund's adjuvant induced arthritis in rats [61]

Arthritis was induced by the sub-plantar injection of 0.1 ml of a freshly prepared suspension of Freund's complete adjuvant (FCA) consisting of 1.0 mg dry heat-killed *Mycobacterium tuberculosis* per millilitre sterile paraffin oil into the left hind paw of rats. Treatment was initiated after 14 days from the day of adjuvant injection. Rats received standard medication (indomethacin/ celecoxib) and compounds (**3c-3e** and **4c-4e**). Swelling of the right hind paw was quantified on 3rd, 6th, 9th, 12th, 15th, 18th and 21st day after the treatment using a digital Vernier calliper. Percent inhibition was calculated, and the difference in the severity of arthritis between the experimental and control groups was statistically analysed.

4.3.7. Assessment of hepatic and renal functions

On the 21st day of the adjuvant-induced arthritis bioassay model, blood was obtained from all groups of rats by puncturing the retro-orbital plexus. Blood samples were allowed to clot at room temperature, and the serum was separated by centrifugation at 2500 rpm for 15 min. Serum was analysed for various biochemical parameters such as Serum Glutamic Oxaloacetate Transaminase (SGOT), Serum Glutamic Pyruvic Transaminase (SGPT), Alkaline phosphatase reflecting hepatic functions; total protein, total albumin collectively reflecting both hepatic as well as renal functions and creatinine and Blood Urea Nitrogen indicating renal functions. Serum analysis was performed using commercial enzyme assay kits (Merck, Germany) as per the manufacturer's instructions.

4.3.8. Ulcerogenic studies

Ulcerogenic liability of the derivatives (**3c-3e** and **4c-4e**) was evaluated on the 21st day of the adjuvant-induced arthritis bioassay. Rats under anaesthesia were sacrificed, and the stomach was removed, opened along the curvature, washed with distilled water and cleaned gently in normal saline. After washing, the stomach mucosa was examined for ulcers using a handheld lens. The lesions were counted, and an ulcer index (UI) for each animal was calculated [62]. It was followed by a histopathological evaluation wherein the stomachs were fixed in 10% v/v formalin and

embedded in paraffin blocks for sectioning. The sections (1-3 mm) were stained with hematoxylin and eosin and photographed using a Nikon digital microscope (Eclipse 200) at 10x magnification.

$$UI = (n \text{ lesion I}) + (n \text{ lesion II})^2 + (n \text{ lesion III})^3$$

Where,

n = number of ulcers

I = ulcer area covering less than 1 mm²

II = ulcer area covering area from 1 to 3 mm² and

III = ulcer area covering more than 3 mm²

4.3.9. Lipid peroxidation study

The extent of lipid peroxidation was determined as per the protocol reported by Ohkawa *et al.* [63]. After the calculation of ulcer index, the gastric mucosa (100 mg) was scraped with two glass slides and homogenised in 1.8 ml of a 1.15% w/v of ice-cold potassium chloride (KCl) solution. The homogenate was supplemented with 0.2 ml of 8.1% sodium dodecyl sulphate (SDS), 1.5 ml of acetate buffer (pH 3.5) and 1.5 ml of 0.8% thiobarbituric acid (TBA). The mixture was then heated at 95 °C for 60 min. After cooling, the reactants were extracted with 5 ml of a mixture comprising of *n*-butanol and pyridine (15:1 v/v), shaken vigorously for 1 min and centrifuged for 10 min at 4000 rpm. The absorbance of the organic supernatant layer was measured at 532 nm, and the results were expressed as nmol MDA 100 mg⁻¹ tissue.

4.3.10. Histopathological assessment of liver and kidney

On the 21st day of the adjuvant-induced arthritis bioassay, rats under anaesthesia were sacrificed, and the liver and kidneys were excised, washed with normal saline and processed through graded alcohol and xylene and embedded in paraffin wax [64]. Sections of 5-6 µm in thickness were cut stained with hematoxylin and eosin. Mounted slides were examined and then photographed using a Nikon digital microscope (Eclipse 200) at 10x magnification.

4.3.11. In vitro COX inhibition assay

The ability of the compounds (**3c-3e** and **4c-4e**) to inhibit ovine COX-1 and COX-2 was evaluated using a colorimetric COX (ovine) inhibitor screening assay kit (catalogue number 760111, Cayman Chemical, Ann Arbor, MI, USA), which utilises the peroxidase component of COX, as per the manufacturer's instructions. The peroxidase activity is assayed colorimetrically by monitoring the appearance of oxidised *N,N,N',N'*-tetramethyl-*p*-phenylenediamine (TMPD) at 590 nm. The concentration of the test compounds producing 50% inhibition (IC₅₀, µM) was calculated from the concentration-inhibition response curve (duplicate determinations).

4.3.12. Enzyme kinetics study [65]

Enzyme kinetics study was performed to assess the nature of inhibition by the derivatives (**3c-3e** and **4c- 4e**) on the COX-2 enzyme. The enzyme kinetics were determined, wherein the arachidonic acid substrate either in the absence or presence of selected derivatives were evaluated at different concentrations between 20-100 μM . The mode of inhibition was determined by following the Lineweaver-Burk double reciprocal plot analysis of the data and calculated as per the Michaelis-Menten kinetics. To understand the possible mode of action, K_m and V_{max} were also calculated. The inhibition constant (K_i) values in the presence of selected derivatives were determined by applying the Cheng-Prusoff equation.

4.3.13. Evaluation of cardiotoxic liability

Cardiotoxicity studies were performed on adult male albino Wistar rats (180-200 g).

Experimental Design: **Group 1:** Normal Control rats treated with 0.3% CMC solution in distilled water (10 ml kg^{-1} , *p.o.*) for 15 days. Initial basal measurement of cTnI and CK-MB in serum was evaluated before treatment. **Group 2:** Isoproterenol control rats administered with ISO (100 mg kg^{-1} , *s.c.*) followed by treatment with 0.3% CMC solution in distilled water (10 ml kg^{-1} , *p.o.*) for 15 days; **Group 3:** ISO + Celecoxib rats administered with ISO (100 mg/ kg^{-1} , *s.c.*) followed by treatment with celecoxib in 0.3% sodium CMC solution for 15 days; **Group 4:** ISO + Comp **3e** rats administered with ISO (100 mg kg^{-1} , *s.c.*) followed by treatment with **3e** in 0.3% sodium CMC solution for 15 days; **Group 5:** ISO + Comp **4c** rats administered with ISO (100 mg kg^{-1} , *s.c.*) followed by treatment with **4c** in 0.3% sodium CMC solution for 15 days. Initial basal measurement of cTnI and CK-MB in serum was evaluated before the start of the experiment. ISO (100 mg kg^{-1} , *s.c.*) was dissolved in saline and injected to rats at an interval of 24 h on day 1 and day 2. ISO induced MI was confirmed by elevated levels of serum cTnI and CK-MB in rat post 24 h of second ISO injection after which the treatment was initiated from the 3rd day and continued till the 18th day.

Blood samples were collected from the retro-orbital plexus. Serum was separated by centrifugation at 4000 rpm for 10 min, and stored at -80°C until assayed. The level of serum cTnI was estimated for both the sets of animals on days 3, 4, 7, 11 and 19 by Electro Chemiluminescence Immunoassay using a standard kit (Roche Diagnostics, Switzerland). Serum CK-MB levels were assayed by commercial kit purchased from Agappe Diagnostics as per the manufacturer's instructions.

4.3.14. Statistical analysis

The experimental results are expressed as the mean \pm S.D (n = 6) followed by a one-way analysis of variance (ANOVA). Tukey's multiple comparisons tests were applied for determining the statistical significance between different groups. Two-way ANOVA followed by a Bonferroni post-test was used for the carrageenan-induced rat paw oedema and adjuvant-induced arthritis bioassays. GraphPad Prism (version 5) was used for all statistical analyses and a p-value < 0.05 was considered significant.

4.4. Computational Studies

4.4.1. *In silico* docking simulations

The docking studies were performed using Schrödinger Glide module in Schrödinger Suite 10.5.014 MM Share Version 3.3.014 Release 2016-1 with workstation 4x Intel(R) Xeon(R) CPU E5-1607 v3 @ 3.10 GHz on Kernel Linux operating environment. The X-ray crystallographic structure of COX-2 complexed with celecoxib (PDB ID: 3LN1) with a resolution of 2.40 Å was retrieved from the Protein Data Bank [66]. GLIDE extra precision (XP) mode was applied to generate favourable ligand poses which were further screened through the filters to examine the spatial fit of the ligand into the COX-2 active site. Protein was prepared using the protein preparation wizard to achieve its lowest energy conformation. This structurally corrected protein was further used for docking analysis. The binding site was generated by keeping the co-crystallized ligand (celecoxib) at the centre of a rectangular box within the protein. A 20 Å grid space was defined for the co-crystallized ligand using the Glide grid module of the software. The LigPrep module was used to generate low-energy conformers for all the ligands. Ligands were kept flexible by generating the ring conformations and by penalising non-polar amide bond structures, whereas the protein was kept rigid throughout the docking studies. All other parameters of the Glide module were maintained at their default values. The lowest energy conformer was selected, and the ligand interactions with the active amino acid residues constituting the COX-2 active site were observed.

4.4.2. MD Simulation

The docked complex of compound **3e** with COX-2 (PDB ID: 3LN1) was further optimised by MD simulation using the Desmond module of Schrödinger Maestro 10.5.014 programme with an OPLS-AA force field in an explicit solvent with the TIP3P water model. The docked complex was soaked adequately in 15727 TIP3P water molecules, and the system was neutralised by adding an appropriate number of chloride counter ions to balance the net charge of the system. The generated solvent model of the docked complex consisted of 56164 atoms. The available system of solvated docked complex was further subjected to energy minimization to maximum 7000 steps of which the first 2000 were steepest descents and the last 5000 were limited-memory Broyden-Fletcher-

Goldfarb-Shanno (L-BFGS). The time step of the simulation was 1.20 nsec, and a 10 Å cut-off was used for non-bonded interactions. The SHAKE algorithm [67] was employed to constrain the bonds involving hydrogen atoms to their equilibrium values. A constant number of atoms, N, volume, V, and temperature, T (NVT) molecular dynamics was performed for the first 100 psec, during which the temperature of the system was raised from 0-300 K. For further simulations, the system was maintained at constant temperature (300 K) and pressure (1.0132 bar). Subsequently, the system was equilibrated at a constant number of atoms, N, pressure, P, and temperature, T (NPT), which consisted of minimization and a short MD simulation (12-24 psec) to relax the model system. Then, a long equilibration MD simulation was performed for 2 nsec, and a long production MD simulation was performed for 5 nsec. Long-range electrostatic interactions were accessed using Particle Mesh Ewald (PME) method.

Conflict of interest

Authors declare no conflict of interest.

Acknowledgements

The authors are grateful to the Head, Department of Chemistry, Institute of Science, Banaras Hindu University (BHU) Varanasi, India for ^1H and ^{13}C -NMR. The authors are grateful to M/s Kekule Pharma Ltd., Hyderabad; M/s GenPharma International Pvt. Ltd., Pune for generously providing celecoxib and indomethacin as gift samples.

References

- [1] M. W. James, C. J. Hawkey, Assessment of non-steroidal anti-inflammatory drug (NSAID) damage in the human gastrointestinal tract, *Br. J. Clin. Pharmacol.* 56 (2003) 146-155.
- [2] V. Schneider, L. E. Levesque, B. Zhang, T. Hutchinson, J. M. Brophy, Association of selective and conventional nonsteroidal antiinflammatory drugs with acute renal failure: A population-based, nested case-control analysis, *Am. J. Epidemiol.* 164 (2006) 881-889.
- [3] D. Adebayo, I. Bjarnason, Is non-steroidal anti-inflammation drug (NSAID) enteropathy clinically more important than NSAID gastropathy, *Postgrad. Med. J.* 82 (2006) 186-191.
- [4] U.S. Food and Drug Administration, Decisional Summary, <http://www.fda.gov/downloads/drugs/drugsafety/postmarketdrugsafetyinformationforpatientsandproviders/ucm106201.pdf> (accessed April 2016)
- [5] P. Singla, V. Luxami, K. Paul, Triazine as a promising scaffold for its versatile biological behavior, *Eur. J. Med. Chem.* 102 (2015) 39-57.

- [6] S. Dadashpour, T. Tuylu Kucukkilinc, O. Unsal Tan, K. Ozadali, H. Irannejad, S. Emami, Design, synthesis and in vitro study of 5,6-diaryl-1,2,4-triazine-3-ylthioacetate derivatives as COX-2 and β -amyloid aggregation inhibitors, *Arch. Pharm. (Weinheim)*. 348 (2015) 179-187.
- [7] H. Irannejad, A. Kebriaieezadeh, A. Zarghi, F. Montazer-Sadegh, A. Shafiee, A. Assadieskandar, M. Amini, Synthesis, docking simulation, biological evaluations and 3D-QSAR study of 5-Aryl-6-(4-methylsulfonyl)-3-(methylthio)-1,2,4-triazine as selective cyclooxygenase-2 inhibitors, *Bioorg. Med. Chem.* 22 (2014) 865-873.
- [8] L. Yurttas, S. Demirayak, S. Ilgin, O. Atlı, In vitro antitumor activity evaluation of some 1,2,4-triazine derivatives bearing piperazine amide moiety against breast cancer cells, *Bioorg. Med. Chem.* 22 (2014) 6313-6323.
- [9] R. Kumar, T. S. Sirohi, H. Singh, R. Yadav, R. K. Roy, A. Chaudhary, S. N. Pandeya, 1,2,4-triazine analogs as novel class of therapeutic agents, *Mini Rev. Med. Chem.* 14 (2014) 168-207.
- [10] L. J. Roberts II, J. D. Morrow, in Goodman & Gilman's The Pharmacological Basis of Therapeutics, ed. J. G. Hardman, L. E. Limbird, McGraw-Hill, 10th edn., Ch. 27 (2001) pp. 716.
- [11] C. S. de Oliveira, B. F. Lira, J. M. Barbosa-Filho, J. G. Lorenzo, P. F. de Athayde-Filho, Synthetic approaches and pharmacological activity of 1,3,4-oxadiazoles: a review of the literature from 2000-2012, *Molecules* 17 (2012) 10192-10231.
- [12] J. Boström, A. Hogner, A. Llinàs, E. Wellner, A. T. Plowright, Oxadiazoles in Medicinal Chemistry, *J. Med. Chem.* 55 (2012) 1817-1830.
- [13] J. Grover, N. Bhatt, V. Kumar, N. K. Patel, B. J. Gondaliya, M. Elizabeth Sobhia, K. K. Bhutania, S. M. Jachak, 2,5-Diaryl-1,3,4-oxadiazoles as selective COX-2 inhibitors and anti-inflammatory agents, *RSC Adv.* 5 (2015) 45535-45544.
- [14] S. Bansal, M. Bala, S. K. Suthar, S. Choudhary, S. Bhattacharya, V. Bhardwaj, S. Singla, A. Joseph, Design and synthesis of novel 2-phenyl-5-(1,3-diphenyl-1*H*-pyrazol-4-yl)-1,3,4-oxadiazoles as selective COX-2 inhibitors with potent anti-inflammatory activity, *Eur. J. Med. Chem.* 80 (2014) 167-174.
- [15] D. V. Dekhane, S. S. Pawar, S. Gupta, M. S. Shingare, C. R. Patil, S. N. Thore, Synthesis and anti-inflammatory activity of some new 4,5-dihydro-1,5-diaryl-1*H*-pyrazole-3-substituted-heteroazole derivatives, *Bioorg. Med. Chem. Lett.* 21 (2011) 6527-6532.
- [16] M. Akhter, N. Akhter, M. M. Alam, M. S. Zaman, R. Saha, A. Kumar, Synthesis and biological evaluation of 2,5-disubstituted 1,3,4-oxadiazole derivatives with both COX and LOX inhibitory activity, *J. Enzyme Inhib. Med. Chem.* 26 (2011) 767-776.

- [17] Y. Li, J. Geng, Y. Liu, S. Yu, G. Zhao, Thiadiazole-a promising structure in medicinal chemistry, *ChemMedChem*. 8 (2013) 27-41.
- [18] A. M. Shkair, A. K. Shakya, N. M. Raghavendra, R. R. Naik, Molecular Modeling, Synthesis and Pharmacological Evaluation of 1,3,4- Thiadiazoles as Anti-inflammatory and Analgesic Agent, *Med. Chem*. 12 (2016) 90-100.
- [19] Y. Song, D. T. Connor, A. D. Sercel, R. J. Sorenson, R. Doubleday, P. C. Unangst, B. D. Roth, V. G. Beylin, R. B. Gilbertsen, K. Chan, D. J. Schrier, A. Guglietta, D. A. Bornemeier, R. D. Dyer, Synthesis, Structure–Activity Relationships, and in Vivo Evaluations of Substituted Di-*tert*-butylphenols as a Novel Class of Potent, Selective, and Orally Active Cyclooxygenase-2 Inhibitors. 2. 1,3,4- and 1,2,4-Thiadiazole Series, *J. Med. Chem.* 42 (1999) 1161-1169.
- [20] A. K. Gadad, M. B. Palkar, K. Anand, M. N. Noolvi, T. S. Boreddy, J. Wagwade, Synthesis and biological evaluation of 2-trifluoromethyl/sulfonamido-5,6-diaryl substituted imidazo[2,1-*b*]-1,3,4-thiadiazoles: A novel class of cyclooxygenase-2 inhibitors. *Bioorg. Med. Chem.* 16 (2008) 276-283.
- [21] D. Kumar, N. Maruthi Kumar, K. H. Chang, K. Shah, Synthesis and anticancer activity of 5-(3-indolyl)-1,3,4-thiadiazoles, *Eur. J. Med. Chem.* 45 (2010) 4664-4668.
- [22] S. Maddila, R. Pagadala, S. B. Jonnalagadda, 1,2,4-Triazoles: A Review of Synthetic Approaches and the Biological Activity, *Lett. Org. Chem.* 10 (2013) 693-714.
- [23] R. Kaur, A. R. Dwivedi, B. Kumar, V. Kumar, Recent Developments on 1,2,4-Triazole Nucleus in Anticancer Compounds: A Review, *Anticancer Agents Med. Chem.* 16 (2016) 465-489.
- [24] H. Cai, X. Huang, S. Xu, H. Shen, P. Zhang, Y. Huang, J. Jiang, Y. Sun, B. Jiang, X. Wu, H. Yao, J. Xu, Discovery of novel hybrids of diaryl-1,2,4-triazoles and caffeic acid as dual inhibitors of cyclooxygenase-2 and 5-lipoxygenase for cancer therapy, *Eur. J. Med. Chem.* 108 (2016) 89-103.
- [25] B. Jiang, Y. Zeng, M.-J. Li, J.-Y. Xu, Y.-N. Zhang, Q.-J. Wang, N.-Y. Sun, T. Lu, X.- M. Wu, Design, synthesis, and biological evaluation of 1,5-diaryl-1,2,4-triazole derivatives as selective cyclooxygenase-2 inhibitors, *Arch. Pharm.* 343 (2010) 500-508.
- [26] B. Jiang, X.-J. Huang, H.-Q. Yao, J.-Y. Jiang, X.-M. Wu, S.-Y. Jiang, Q.-J. Wang, T. Lu, J.-Y. Xu, Discovery of potential anti-inflammatory drugs: diaryl-1,2,4-triazoles bearing *N*-hydroxyurea moiety as dual inhibitors of cyclooxygenase-2 and 5-lipoxygenase, *Org. Biomol. Chem.* 12 (2014) 2114-2127.
- [27] A. G. Banerjee, N. Das, S. A. Shengule, R. S. Srivastava, S. K. Srivastava, Synthesis, characterization, evaluation and molecular dynamics studies of 5, 6-diphenyl-1,2,4-triazin-

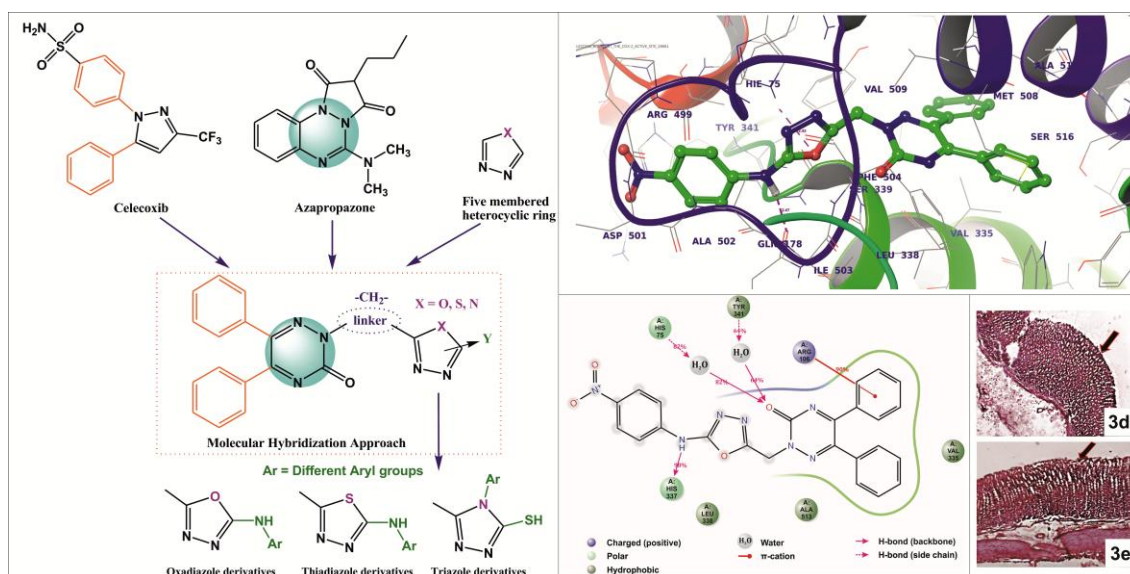
- 3(2*H*)-one derivatives bearing 5-substituted 1,3,4-oxadiazole as potential anti-inflammatory and analgesic agents, *Eur. J. Med. Chem.* 101 (2015) 81-95.
- [28] V. R. Solomon, C. Hu, H. Lee, Hybrid pharmacophore design and synthesis of isatin-benzothiazole analogs for their anti-breast cancer activity, *Bioorg. Med. Chem.* 17 (2009) 7585-7592.
- [29] B. Meunier, Hybrid Molecules with a Dual Mode of Action: Dream or Reality, *Acc. Chem. Res.* 41 (2008) 69-77.
- [30] S. K. Bhanot, M. Singh, N. R. Chatterjee, The chemical and biological aspects of fluoroquinolones: reality and dreams, *Curr. Pharm. Des.* 7 (2001) 311-335.
- [31] V. V. Kouznetsov, A. Gomez-Barrio, Recent developments in the design and synthesis of hybrid molecules based on aminoquinoline ring and their antiplasmodial evaluation, *Eur. J. Med. Chem.* 44 (2009) 3091-3113.
- [32] J. Adamec, R. Beckert, D. Weiss, V. Klimesova, K. Waissner, U. Mollmann, J. Kaustova, V. Buchta, Hybrid molecules of estrone: New compounds with potential antibacterial, antifungal, and antiproliferative activities, *Bioorg. Med. Chem.* 15 (2007) 2898-2906.
- [33] A. G. Banerjee, L. P. Kothapalli, P. A. Sharma, A. B. Thomas, R. K. Nanda, S. K. Shrivastava, V. V. Khatanglekar, A facile microwave assisted one pot synthesis of novel xanthene derivatives as potential anti-inflammatory and analgesic agents, *Arab. J. Chem.* (2011) DOI: 10.1016/j.arabjc.2011.06.001.
- [34] A. Kulshrestha, N. Das, A. G. Banerjee, S. K. Shrivastava, Design, synthesis and pharmacological evaluation of some pyrazolopyrimidin-6(7*H*)-ones and tricyclic 8-oxo-dihydrooxazolopyrazolopyrimidin-9-ium chloride derivatives, *Arab. J. Chem.* (2014) DOI: 10.1016/j.arabjc.2014.03.012.
- [35] L. A. Williams, A. O'Connar, L. Latore, O. Dennis, S. Ringer, J. A. Whittaker, J. Conrad, B. Vogler, H. Rosner, W/ Kraus, The in vitro anti-denaturation effects induced by natural products and non-steroidal compounds in heat treated (immunogenic) bovine serum albumin is proposed as a screening assay for the detection of anti-inflammatory compounds, without the use of animals, in the early stages of the drug discovery process, *West Indian Med. J.* 57 (2008) 327-331.
- [36] E. L. Opie, On the relation of necrosis and inflammation to denaturation of proteins, *J. Exp. Med.* 115 (1962) 597-608.
- [37] N. H. Grant, H. E. Alburn, C. Kryzanasuska, Stabilization of serum albumin by anti-inflammatory drugs. *Biochem. Pharmacol.* 19 (1970) 715-722.

- [38] S. E. Haque, M. Tauseef, Effect of aspirin and celecoxib on lens glutathione and soluble protein profile in naphthalene induced cataract in Wistar rats. *J. Pharm. Res.* 10 (2016) 270-274.
- [39] B. Silvestrini, A. Guglielmotti, L. Saso, C. Y. Cheng, Changes in concanavalin A-reactive proteins in inflammatory disorders, *Clin. Chem.* 35 (1989) 2207-2211.
- [40] B. Marzouk, Z. Marzouk, E. Haloui, N. Fenina, A. Bouraoui, M. Aouni, Screening of analgesic and anti-inflammatory activities of *Citrullus colocynthis* from southern Tunisia, *J. Ethnopharmacol.* 128 (2010) 15-19.
- [41] Y. Ozaki, Antiinflammatory effect of *Curcuma xanthorrhiza* Roxb, and its active principles, *Chem. Pharm. Bull.* 38 (1990) 1045-1048.
- [42] L. J. Garcia, L. Hamamura, M. P. Leite, S. M. Rochae, Pharmacological analysis of the acute inflammatory process induced in the rat's paw by local injection of carrageenin and by heating, *Br. J. Pharmacol.* 48 (1973) 88-96.
- [43] A. Panthong, D. Kanjanapothi, T. Taesotikul, T. Wongcome, V. Reutrakul, Anti-inflammatory and antipyretic properties of *Clerodendrum petasites* S. Moore, *J. Ethnopharmacol.* 85 (2003) 151-156.
- [44] J. S. Courtenay, M. J. Dallman, A. D. Dayan, A. Martin, B. Mosedale, Immunisation against heterologous type II collagen induces arthritis in mice, *Nature.* 283 (1980) 666-668.
- [45] T. Pohle, T. Brzozowski, J. C. Becker, I. R. Vander Voort, A. Markmann, S. J. Konturek, A. Moniczewski, W. Domschke, J. W. Konturek, Role of reactive oxygen metabolites in aspirin-induced gastric damage in humans: gastroprotection by vitamin C, *Aliment Pharmacol. Ther.* 15 (2001) 677-687.
- [46] P. K. Nigam, Biochemical markers of myocardial injury. *Ind. J. Clin. Biochem.* 22 (2007) 10-17.
- [47] M. P. P. Stanely, A. J. Roy, p-Coumaric acid attenuates apoptosis in isoproterenol-induced myocardial infarcted rats by inhibiting oxidative stress, *Int. J. Cardiol.* 168 (2013) 3259-3266.
- [48] M. Kumar, E. R. Kasala, L. N. Bodduluru, V. Dahiya, M. Lahkar, Baicalein protects isoproterenol induced myocardial ischemic injury in male Wistar rats by mitigating oxidative stress and inflammation, *Inflamm. Res.* 65 (2016) 613-622.
- [49] M. M. Kannan, S. D. Quine, Ellagic acid inhibits cardiac arrhythmias, hypertrophy and hyperlipidaemia during myocardial infarction in rats, *Metabolism.* 62 (2013) 52-61.
- [50] M. Kumar, E. R. Kasala, L. N. Bodduluru, V. Dahiya, D. Sharma, V. Kumar, M. Lahkar, Animal models of myocardial infarction: Mainstay in clinical translation, *Regul. Toxicol. Pharmacol.* 76 (2016) 221-230.

- [51] M. Kontoyianni, L. M. McClellan, G. N. Sokol, Evaluation of Docking Performance: Comparative Data on Docking Algorithms, *J. Med. Chem.* 47 (2004) 558-565.
- [52] C. A. Lipinski, F. Lombardo, B. W. Dominy, P. J. Feeney, Experimental and computational approaches to estimate solubility and permeability in drug discovery and development settings. *Adv. Drug Deliv. Rev.* 46 (2001) 3–26.
- [53] D. F. Veber, S. R. Johnson, H. Y. Cheng, B. R. Smith, K. W. Ward, K. D. Kapple, Molecular Properties That Influence the Oral Bioavailability of Drug Candidates, *J. Med. Chem.* 45 (2002) 2615-2623.
- [54] R. M. Abdel-Rahman, M. Fawzy, Y. Gabr, S. G. Abdel-Hamide, M. S. Abdel-Tawab, Nucleophilic substitution and ring closure of carboxyhydrazide bearing 3-oxo-5,6-diphenyl-1,2,4-triazin-2-yl-moiety, *Ind. J. Heterocycl. Chem.* 3 (1994) 281-286.
- [55] S. O. Podunavac-kuzmanovic, D. D. Cvetkovic, D. J. Barna, The effect of lipophilicity on the antibacterial activity of some 1-benzylbenzimidazole derivatives, *J. Serb. Chem. Soc.* 73 (2008) 967-978.
- [56] C. Kilkenny, W. J. Browne, I. C. Cuthill, M. Emerson, D. G. Altman, Improving Bioscience Research Reporting: The ARRIVE Guidelines for Reporting Animal Research, *PLOS Biol.* 8 (2010) e1000412.
- [57] B. Ramesh, C. M. Bhalgat, Novel dihydropyrimidines and its pyrazole derivatives: Synthesis and pharmacological screening, *Eur. J. Med. Chem.* 46 (2011) 1882-1891.
- [58] OECD. Test No. 425: Acute Oral Toxicity: Up-and-Down Procedure, OECD Guidelines for the Testing of Chemicals, Section 4, (2008) OECD Publishing, Paris. DOI: <http://dx.doi.org/10.1787/9789264071049-en>
- [59] C. A. Winter, E. A. Risley, G. W. Nuss, Carrageenin-induced edema in hind paw of the rat as an assay for antiinflammatory drugs, *Proc. Soc. Exp. Biol. Med.* 11 (1962) 544-547.
- [60] P. Chattopadhyay, S. E. Besra, A. Gomes, M. Das, P. Sur, S. Mitra, J. R. Vedasiromoni, Anti-inflammatory activity of tea (*Camellia sinensis*) root extract, *Life Sci.* 74 (2004) 1839-1849.
- [61] R. M. Latha, T. Geetha, P. Varalakshmi, Effect of *Vernonia cinerea* Less Flower Extract in Adjuvant-Induced Arthritis, *Gen. Pharmacol.-Vasc. S.* 31 (1998) 601-606.
- [62] I. Szelenyi, K. Thiemer, Distention ulcer as a model for testing of drugs for ulcerogenic side effects, *Arch. Toxicol.* 41 (1978) 99-105.
- [63] H. Ohkawa, N. Ohishi, K. Yagi, Assay for lipid peroxides in animal tissues by thiobarbituric acid reaction, *Anal. Biochem.* 95 (1979) 351-358.
- [64] A. E. Galigher, E. N. Kozloff, in *Essentials of Practical Microtechnique*, ed. Lea and Febiger, Hagerstown Publications, Maryland, U.S.A, 2nd edn., Vol. 20 (1971) pp. 77.

- [65] H. Lineweaver, D. J. Burk, The Determination of Enzyme Dissociation Constants, *J. Am. Chem. Soc.* 56 (1934) 658-666.
- [66] J. L. Wang, D. Limburg, M. J. Graneto, J. Springer, J. R. B. Hamper, S. Liao, J. L. Pawlitz, R. G. Kurumbail, T. Maziasz, J. J. Talley, J. R. Kiefer, J. Carter, The novel benzopyran class of selective cyclooxygenase-2 inhibitors. Part 2: The second clinical candidate having a shorter and favorable human half-life, *Bioorg. Med. Chem. Lett.* 20 (2010) 7159-7163.
- [67] J. P. Ryckaert, G. Ciccotti, H. J. C. Berendsen, Numerical integration of the Cartesian Equations of Motion of a System with Constraints: Molecular Dynamics of n-Alkanes, *J. Comp. Physiol.* 23 (1977) 327-341.

Graphical abstract



Highlights:

- Fifteen novel hybrids designed for selective COX-2 inhibition.
- Compounds **3c-3e** and **4c-4e** exhibited selective COX-2 inhibition.
- Importance of additional –NH linker exemplified.
- Potential hybrids bereft of ulcerogenic, hepatic, renal and cardiotoxic liability.
- Molecular docking and dynamic study corroborated consensual interaction with COX-2.

ACCEPTED MANUSCRIPT